

## CHAPTER 46

# CORRELATION OF WATER LEVEL VARIATIONS WITH WAVE FORCES ON A VERTICAL PILE FOR NONPERIODIC WAVES

Robert O. Reid

Associate Professor, Department of Oceanography and Meteorology  
Texas A. & M. College, College Station, Texas.

### ABSTRACT

This paper describes the design and application of numerical transforms for the estimation of the field of motion associated with irregular, non-periodic surface waves from measured serial sequences of water level at a fixed point. The design of these transforms is based upon the linear theory for long-crested waves. The method is applied in the analysis of wave forces exerted upon a vertical circular cylinder, where the measured reaction is considered to be expressible as a linear combination of two independent functions of time. One of these functions depends (nonlinearly) upon the velocity field, the other depends (linearly) upon the acceleration field. The covariance of these functions with the measured reaction allows a direct means of evaluation of the drag and inertial coefficients for the cylinder.

### 1. INTRODUCTION

In the analysis of records of forces exerted upon structures by ocean waves it is desirable to have an accurate and objective means of deducing the field of fluid motion so as to provide the necessary kinematic information for a reliable evaluation of the drag and inertial coefficients associated with such forces. In field tests, direct measurement of the distribution of fluid motion associated with waves is not as yet a feasible means of providing the detailed information desired. Even in laboratory wave tests the direct measurement of particle velocities is difficult. On the other hand, direct measurement of water level variations at a fixed point can be carried out with relative ease, in both laboratory and field tests. If the waves are simple harmonic and periodic, or closely approximate this condition, then the amplitude and period of the surface variations, together with the known depth of water, will allow the estimation of the desired particle velocity and acceleration field through the use of classical wave theory. The orbital currents so deduced plus the simultaneous records of wave forces on the object in question will allow an estimation of the drag and inertial coefficients. In

---

<sup>1</sup> Contribution from the Department of Oceanography and Meteorology, Agricultural and Mechanical College of Texas, Oceanography and Meteorology Series No. 101.

## COASTAL ENGINEERING

effect one is really correlating a record of water level variations with wave force variations through the medium of the wave theory and deducing therefrom two linearly independent regression coefficients. This method has precedent in the studies carried out in the laboratory at the University of California (Morison, et.al., 1950) and has been utilized in a number of later laboratory studies. Controlled conditions of wave generation allow the attainment of nearly simple harmonic waves and the foregoing method of analysis is therefore ideally suited to measurements carried out in the laboratory.

In most field studies on the other hand it is generally the case that the waves are neither simple harmonic nor periodic. Instead the waves are characterized by a continuous spectrum which covers a broad range of periods. The resulting water level variations and serial sequences of forces are highly complicated and constitute what might be termed filtered noise. With the exception of certain cases of very regular swell, as may occur at times on the west coast of the United States or the Atlantic coast of Europe during the northern summer, it is virtually impossible to pick out a characteristic period and amplitude for the waves, other than from a statistical standpoint. The statistical mean "period" and mean amplitude for a given wave train are useful from the standpoint of gross classification of the waves, but these quantities are hardly sufficient from the standpoint of the details or even the statistics of the fluid motion or pressure field associated with the wave train in a given depth of water. It is known for example that the mean "periods" of waves as deduced from pressure measurements at the bottom in shallow water do not coincide with mean "periods" as deduced from direct surface measurements. Furthermore, if the mean amplitude of the pressure variation is converted to an equivalent amplitude of water level variation based upon the mean "period" of the pressure variations, the equivalent amplitude is not the same as the mean amplitude of the measured surface waves, unless the waves possess a very narrow spectrum. The difference in wave statistics deduced from pressure gages and from direct surface measurements is borne out strikingly in the recent studies at Berkeley (Wiegel and Kukk, 1957).

Much of the discrepancy can be accounted for on the basis of the continuous nature of the spectrum of the waves and proper utilization of the wave theory in the conversion of pressure records to equivalent surface records or visa versa [see for example Fuchs (1952)]. The conversion of water level variations to pressure variations at the bottom can be effected by means of a special numerical filter which is designed on the basis of the linear wave theory. If we regard the surface profile as the resultant of many simple harmonic waves of different amplitudes, periods and relative phases, then the filter when properly constructed acts upon each of those components simultaneously and adjusts the amplitude according to the period of each individual component without altering the relative phase. The output of the filter is the resultant of all the adjusted wave components. The numerical filter for pressure simply simulates the hydrodynamic filtering as predicted by the linear theory. The advantage of the system is that it can be utilized for the most complex wave records.

# CORRELATION OF WATER LEVEL VARIATIONS WITH WAVE FORCES ON A VERTICAL PILE FOR NONPERIODIC WAVES

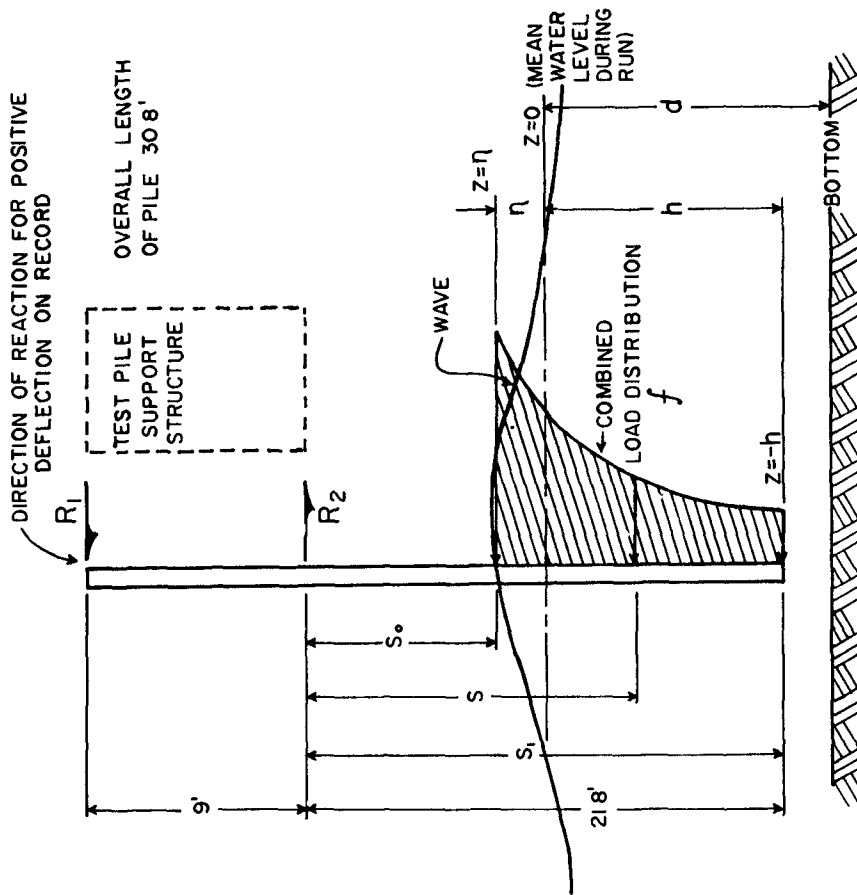


Fig. 2. Schematic of loads on test pile.

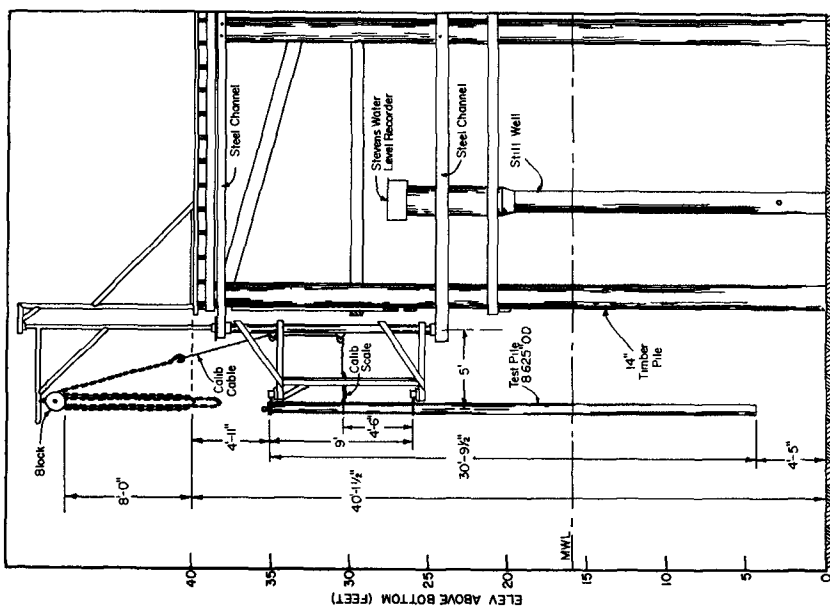


Fig. 1. Scaled drawings of wave force installation at Sun Oil Company Pier, Caplen, Texas. The steel test pile was located on the southeast corner of the platform one-half mile from shore. The directional orientation of the pile support could be varied through an angle of  $180^\circ$ .

# COASTAL ENGINEERING

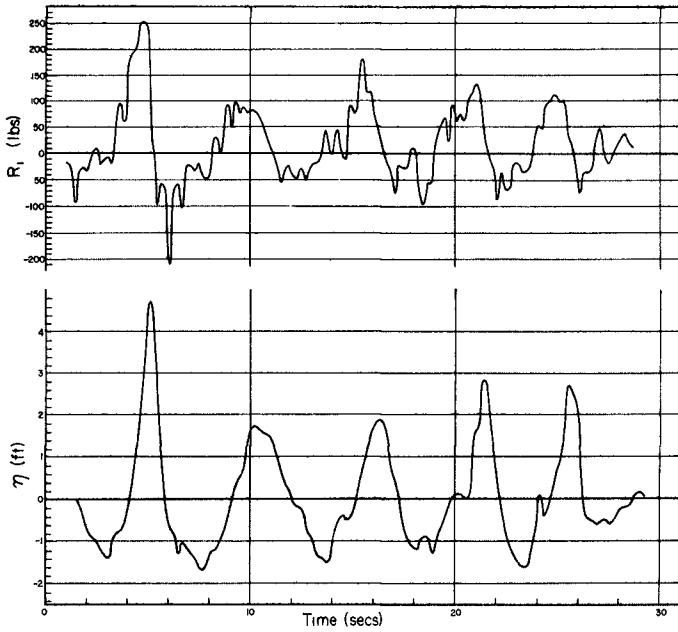


Fig. 3. Sample of serial sequences of  $\eta$  and reaction  $R_1$  (Run 7).

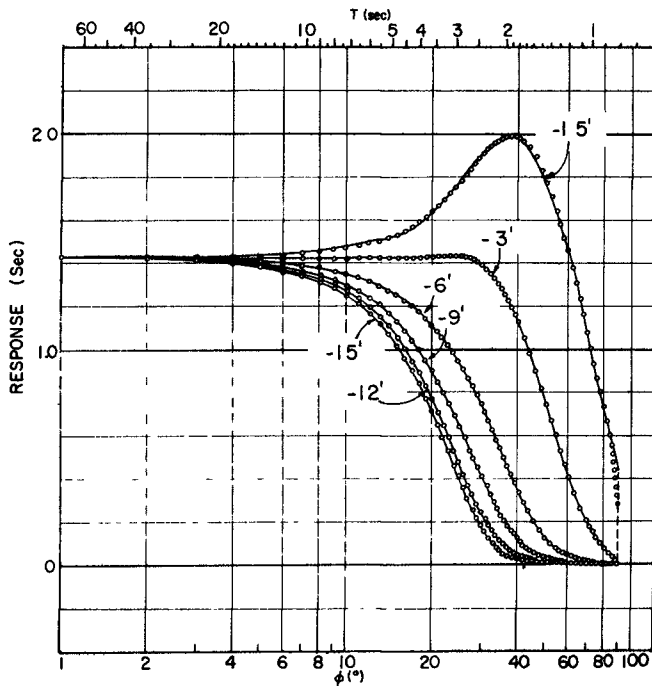


Fig. 4. Response Diagram for  $u$  at Subsurface Levels. Full curves are response from linear wave theory, circled points are derived from Eq. (36) using the  $a_n$  values from Table II. Vertical dashed line is the design "cut-off" position ( $\phi=90^\circ$  or  $T=0.8$  sec). For a simple harmonic wave of period  $T$  and amplitude  $A$ , the amplitude of velocity  $u$  at depth  $z$  is equal to  $A$  times the response factor.

# CORRELATION OF WATER LEVEL VARIATIONS WITH WAVE FORCES ON A VERTICAL PILE FOR NONPERIODIC WAVES

Numerical filters or transforms can also be constructed for ascertaining the serial sequence of velocity and acceleration of fluid at a given depth using the measured water level variations as input. In the case of acceleration the numerical transform must be such as to allow for a shift in phase for each component in the water level sequence. The following report discusses the design and application of such transforms. A specific set of measurements of waves and wave forces on a vertical cylinder in the Gulf of Mexico is utilized to illustrate the method of analysis of the field of motion and of the drag and inertial coefficients deduced from this field of motion and the measured forces.

## 2. WAVE FORCE FIELD EXPERIMENT

Measurements of wave forces on a smooth vertical pile of 8.625 inches diameter associated with irregular waves of about 2 to 4 feet significant height and about 3.5 to 5 seconds mean "period" were carried out at the Sun Oil Company pier at Caplen,<sup>2</sup> Texas, as part of a project sponsored by the Bureau of Yards and Docks. A scaled drawing of the installation is given in Fig. 1. The test pile was supported at two positions nine feet apart by means of "U" bolts attached to flexure bars. The pile was submerged to a nominal depth of about 12 feet in sea water of about 16 feet total depth at mean tide level. Measurements of the reaction  $R_1$ , at the upper level (see Fig. 2) were obtained simultaneously with movie film records of the water level variations at the pile position, the pile being marked in one foot intervals. The pile support could be rotated into the waves so as to obtain the maximum thrust normal to the instrumented flexure bars. Details of the measuring system, the calibration of the system and the listings of basic data are contained in technical reports of the project (Reid, 1954, 1956). Essentially the reaction was measured by means of the calibrated output of SR-4 strain gages mounted on the flexure bars which supported the pile. Unfortunately only the upper level measurements were satisfactory so that it was not possible to ascertain experimentally both the total wave load and the effective center of action of the wave load by two separate reactions  $R_1$  and  $R_2$  as originally planned. However, the measurement of  $R_1$  alone can be utilized in the estimation of the drag and inertial coefficients. Measurements of wind velocity, wave direction, tide elevation and mean surface currents were obtained as supplementary information.

A typical sequence of measurements of water level and reaction are shown in Fig. 3. Positive  $R_1$  represents reaction in the direction of wave propagation (see Fig. 2). The water level anomaly,  $\eta$ , was estimated from the film records to the nearest 0.1 foot. The relative error in water level anomaly is estimated as about  $\pm 0.05$  foot and that of  $R_1$  as about  $\pm 5$  lbs.

---

<sup>2</sup> Caplen is located about 30 miles east of Galveston on the Bolivar Peninsula. The installation was located at the end of the pier which extends about 1/2 mile into the Gulf of Mexico.

## COASTAL ENGINEERING

However, the zero reference for  $R_1$  is subject to a much larger error, and is considered as one of the unknowns in the analysis. All tabulations of  $\eta$  and  $R_1$  were carried out at intervals of 0.2 second from the original records. Time checks were provided in the film records to insure proper interpolation and alignment with the records of  $R_1$ . A total of 570 seconds of record consisting of 18 separate runs were analyzed. The longest single run was about 46 seconds. The range of wind speeds was 10 to 30 mph during the different series of runs.

A schematic of the loads on the test pile accompanying the passage of a wave is indicated in Fig. 2. In the absence of vibration of the pile and its supporting platform, a quasi-static balance of the moments of load on the test pile must exist. Taking moments about the position of the lower support gives:

$$bR_1(t) = \int_{s_0}^{s_1} s f(s, t) ds \quad (1)$$

where  $s$  is the vertical distance below the lower support,  $b$  is the vertical distance between the two supports and  $f$  is the wave load per unit length of pile at position  $s$  and time  $t$ . It is assumed that the moment induced by the "U" bolt connection at each support is negligible. The static balance of moments should be adequate as long as the spectral energy associated with  $\eta(t)$  is confined to periods in excess of the natural periods of vibration of the test pile and/or supporting structure, such that resonant conditions are not excited. If this is not the case then the platform and pile accelerations can become significant and should therefore be taken into account if the records of  $R_1$  are used directly. An alternative is to apply Eq.(1) to records of  $R_1$  from which the energy associated with vibrational resonance or near resonance has been effaced, provided that the same range of periods are suppressed in the estimated wave load  $f$ . In the measurements utilized here, vibrational periods were present and the suppression of these vibrations was carried out objectively by use of a numerical filter which is described in a later section. The vibrational periods were approximately 0.5 and 1.1 seconds. Evidence of these periods can be seen in the unfiltered record of  $R_1$  shown in Fig. 3. The amplitudes associated with these periods in the  $R_1$  record are disproportionately large as compared with the relative energy associated with these same periods in the simultaneous water level record. Consequently unless these vibrations are effaced from the record, it is apparent that significant errors in the estimates of drag and inertial coefficients associated with  $f$  can result.

CORRELATION OF WATER LEVEL VARIATIONS WITH WAVE  
FORCES ON A VERTICAL PILE FOR NONPERIODIC WAVES

3. THE WAVE LOAD REGRESSION FORMULA

Following Morison, et.al. (1950), it is presumed that the wave load per unit length on the vertical cylinder can be expressed in the form

$$f = C_D \frac{w}{2g} D |v|v + C_M \frac{w}{g} \frac{\pi}{4} D^2 \dot{v} \quad (2)$$

where  $v$  and  $\dot{v}$  are respectively the horizontal components of fluid velocity and acceleration in the vicinity of the pile at level  $s$  and time  $t$ ,  $w$  is the specific weight of sea water (64 lbs/cuft),  $D$  the pile diameter,  $g$  the acceleration due to gravity, and  $C_D$  and  $C_M$  are the dimensionless drag and inertial coefficients respectively. The latter coefficients are regarded as constants for any particular sequence of waves. In this sense Eq.(2) is really a regression formula to which the observed data are to be fitted in such a way as to give the best estimate of  $f$  in a least squares sense. However, Eq.(2) is not directly applicable since both  $f$  and  $v$  are unknown.

The field of velocity and acceleration can be deduced from the observed sequence of water level anomaly and a knowledge of the steady currents upon which the waves are superimposed. The measured reaction on the other hand gives an estimate of the moment of the total wave load according to Eq.(1). Using relations (1) and (2) jointly it is possible, in the absence of vibrations, to represent the reaction  $R_1$  in the form

$$R_1(t) = C_D F_1(t) + C_M F_2(t) \quad (3)$$

where  $F_1(t)$  and  $F_2(t)$  are defined by

$$F_1 \equiv \frac{wD}{2g} \left\{ \left[ \frac{L-h}{b} - 1 \right] \int_{-h}^{\eta} |v|v \, dz - \frac{1}{b} \int_{-h}^{\eta} z |v|v \, dz \right\} \quad (4)$$

and

$$F_2 \equiv \frac{\pi}{4} \frac{wD^2}{g} \left\{ \left[ \frac{L-h}{b} - 1 \right] \int_{-h}^{\eta} \dot{v} \, dz - \frac{1}{b} \int_{-h}^{\eta} z \dot{v} \, dz \right\} \quad (5)$$

where  $L$  is the pile length,  $h$  is the depth of submergence of the pile below still water level,  $\eta$  is the instantaneous elevation of the sea surface above still water level, and  $z$  is the vertical coordinate taken positive upwards from still water level. The value of  $h$  of course depends upon the state of the tide.

The velocity  $v$  can be expressed in the form

$$v = U + u \quad (6)$$

## COASTAL ENGINEERING

where  $U$  is the steady current at level  $z$  and  $u$  is the component of motion at  $z, t$  associated directly with the waves. It is evident that there is no contribution of the steady current to the acceleration so that  $\dot{v} = \dot{u}$ . For simplicity in notation we will hereafter replace the velocity product  $|v|v$  by  $p$ . Thus

$$p = |U + u| \cdot (U + u), \quad (7)$$

which is directly related to the drag pressure, but has the units  $\text{ft}^2/\text{sec}^2$ . Note that  $p$  has the sign of the sum  $U + u$ , and that the mean value of  $p$  over a long time interval is not zero even though the average of  $u, \dot{u}$  and  $\eta$  is zero. Because of this we should expect to find that the mean value of  $R_1$  differs from zero.

In view of the fact that  $u$  enters in a quadratic manner in Eq.(4) it is necessary to evaluate  $u$  at several levels and employ an appropriate summation to approximate the integrals. Let the constant  $h_0$  represent a nominal depth of submergence (12 feet for the present example) and consider the range  $0$  to  $-h_0$  divided into four equal intervals of size  $\Delta z$ . The integrals in Eq.(4) can then be approximated as follows:

$$\int_{-h}^{\eta} |v|v \, dz \doteq \frac{\Delta z}{3} [p_0 + 4p_1 + 2p_2 + 4p_3 + p_4] + (h - h_0)p_4 + \eta p_0 + \frac{1}{2} \eta^2 \frac{\Delta p_0}{\Delta z} \quad (8)$$

and

$$- \int_{-h}^{\eta} z |v|v \, dz \doteq \frac{4}{3} (\Delta z)^2 [p_1 + p_2 + 3p_3 + p_4] + \frac{1}{2} (h^2 - h_0^2) p_4 - \frac{1}{2} \eta^2 p_0 - \frac{1}{3} \eta^3 \frac{\Delta p_0}{\Delta z} \quad (9)$$

where the subscripts indicate the elevation in the sense that  $p_j$  is the value of  $p$  at  $z = -j\Delta z$  (relative to still water level), and  $\Delta p_0$  is defined by

$$\Delta p_0 \equiv p\left[-\frac{\Delta z}{2}, t\right] - p\left[-\frac{\Delta z}{2}, t\right] \quad (10)$$

Simpson's rule has been applied for the interval  $-h_0$  to  $0$  in the above approximations. A generalization of this procedure for any even number of intervals is easily made.

**CORRELATION OF WATER LEVEL VARIATIONS WITH WAVE  
FORCES ON A VERTICAL PILE FOR NONPERIODIC WAVES**

In the case of Eq.(5), the acceleration enters linearly and it is possible to evaluate the major portion of the integrals (for the range  $-h_0$  to 0) directly from the water level variations as we shall see presently. Consequently the complete integrals in Eq.(5) can be approximated as follows :

$$\int_{-h}^{\eta} \dot{v} dz \doteq \int_{-h_0}^{\eta} \dot{u} dz + (h - h_0) \dot{u}_4 + \eta \dot{u}_0 + \frac{1}{2} \eta^2 \left[ \frac{\partial \dot{u}}{\partial z} \right]_0 \quad (11)$$

$$- \int_{-h}^{\eta} z \dot{v} dz \doteq \int_{-h_0}^{\eta} |z| \dot{u} dz + \frac{1}{2} (h^2 - h_0^2) \dot{u}_4 - \frac{1}{2} \eta^2 \dot{u}_0 - \frac{1}{3} \eta^3 \left[ \frac{\partial \dot{u}}{\partial z} \right]_0 \quad (12)$$

where the subscripts have the same meaning as in Eqs.(8) and (9). Thus  $\dot{u}_4$  is the acceleration at  $z = -h_0$ . The last term in each of the Eqs.(8) to (12) is a secondary correction term to take into account the effect of the gradient of  $p$  and  $\dot{u}$  near the surface.

Eq.(3) is a linear regression equation for  $R_1$  in terms of the linearly independent functions  $F_1$  and  $F_2$ . The function  $F_1$  can be expressed as a linear combination of  $p_j$  functions with the coefficients of some of the terms being polynomials in  $\eta$ . The function  $F_2$  can be expressed as a linear combination of  $\dot{u}_n$  and linear integral operations on  $\dot{u}$  but again the coefficients of some of the terms are polynomials in  $\eta$ . Since  $u$  and  $\dot{u}$  can be expressed in terms of the sequence  $\eta(t)$ , it follows that  $F_1$  and  $F_2$  depend primarily upon the sequence  $\eta$ . In addition  $F_1$  depends upon  $U(z)$  and both functions depend upon the slowly changing value of  $h$ . The functional dependence of  $F_1$  and  $F_2$  on the sequence  $\eta(t)$  is nonlinear and in the case of the "drag" function,  $F_1$ , the dependence on  $\eta(t)$  is strongly nonlinear. This implies that the spectrum of the function  $\eta(t)$  cannot be converted to the spectrum of  $F_1(t)$  by a simple linear transformation. Some of the spectral energy at and near frequency  $\omega$  in the record of  $\eta(t)$  will show up as energy with frequency at or near  $2\omega$  and zero frequency in the spectrum of  $F_1(t)$ . Furthermore there will be interaction of the spectral components such that frequencies of absolute value  $\omega_1$  and  $\omega_2$  in the record of  $\eta(t)$  can produce frequencies of  $\omega_1 + \omega_2$  and  $|\omega_1 - \omega_2|$  in the spectrum of  $F_1(t)$ . This is also true in respect to the "inertial" function  $F_2(t)$ , but the amount of nonlinear dispersion of energy in the spectrum is less pronounced since the primary contribution to the function is from linear transformations of  $\eta$ , through  $\dot{u}$ . The possibility of producing low frequencies  $|\omega_1 - \omega_2|$  in either function, and particularly in  $F_1(t)$ , from high frequencies of nearly the same value, is a point to be borne in mind in respect to the final analysis of  $F_1(t)$  and  $F_2(t)$ .

It is clear that once  $F_1(t)$  and  $F_2(t)$  are determined, the regression coefficients  $C_D$  and  $C_M$  in Eq.(3) can be evaluated by a suitable least squares

## COASTAL ENGINEERING

fit procedure employing the measured sequences of  $R_1$ . This matter is discussed in some detail in section 8.

### 4. NON-PERIODIC WAVES

Any wave record of finite duration, extending from time  $t_1$  to  $t_2$ , can be represented in the form of a Fourier integral as follows

$$\eta(t) = \int_0^{\infty} M(\omega) \cos [\omega t - \Theta(\omega)] d\omega \quad (13)$$

where the functions  $M(\omega)$  and  $\Theta(\omega)$  can be evaluated from the relations

$$M \cos \Theta = \frac{1}{\pi} \int_{t_1}^{t_2} \eta(t) \cos \omega t dt \quad (14)$$

$$M \sin \Theta = \frac{1}{\pi} \int_{t_1}^{t_2} \eta(t) \sin \omega t dt \quad (15)$$

The quantities  $M(\omega)$  and  $\Theta(\omega)$  are real functions of the frequency parameter  $\omega$  and jointly characterize the finite sequence of  $\eta$  at some fixed location. The quantity  $E = M^2(\omega)/(t_2 - t_1)$  represents the energy spectral function for the finite  $\eta$  sequence and has the important property

$$\int_0^{\infty} E(\omega) d\omega = \overline{\eta^2} \quad (16)$$

where the bar indicates a time average for the period  $t_1$  to  $t_2$ . This is a direct result of Parseval's theorem in connection with Fourier Integrals. It follows that one system of evaluating the energy spectrum is to subject the record  $\eta(t)$  to narrow band pass filters<sup>3</sup> and evaluate the mean square value of the output of each filter.

The waves represented by (13) are not periodic. However, in the special case where the major portion of the spectral energy is concentrated in a narrow band centered at some modal frequency  $\omega_0$ , the disturbance  $\eta$  manifests itself in the form of an amplitude modulated wave train with a quasi-periodic carrier wave of mean frequency  $\omega_0$ . The statistical properties of waves

---

<sup>3</sup> It is implied here that the filter leaves the energy unaffected for those frequencies in a small band  $\Delta\omega$  centered at frequency  $\omega$  and eliminates the energy associated with all other frequencies.

# CORRELATION OF WATER LEVEL VARIATIONS WITH WAVE FORCES ON A VERTICAL PILE FOR NONPERIODIC WAVES

whose spectrum is narrow, and for which the phase parameter  $\Theta$  is random, has been studied analytically by Longuet-Higgins (1952). However, in many cases the wave spectrum is not narrow; this is particularly true of wind waves in the process of generation. The records for waves possessing a broad spectrum resemble filtered noise and do not possess any distinct periodicity (see Fig. 3). However, the record can always be represented by an equation of the type (13).

If the waves are long-crested, and of small amplitude then it follows<sup>4</sup> from the linear theory of irrotational motion associated with waves in water of constant depth that

$$u(z, t) = \int_0^{\infty} M(\omega) \left\{ \omega \frac{\cosh k(z+d)}{\sinh kd} \right\} \cos [\omega t - \Theta(\omega)] d\omega \quad (17)$$

and

$$\dot{u}(z, t) = - \int_0^{\infty} M(\omega) \left\{ \omega^2 \frac{\cosh k(z+d)}{\sinh kd} \right\} \sin [\omega t - \Theta(\omega)] d\omega \quad (18)$$

where  $k$  is the wave number and is related to the frequency  $\omega$  by the formula

$$\omega^2 = gk \tanh kd \quad (19)$$

The evaluation of  $k$  in terms of  $\omega$  is facilitated by the use of Wiegel's Tables (1954). There the notation  $T = 2\pi/\omega$  and  $L = 2\pi/k$  for period and wave length is employed.

Formulas (17) and (18) hold provided that the mean square slope which is specified by

$$\int_0^{\infty} k^2 E(\omega) d\omega \quad (20)$$

is sufficiently small compared with unity, and provided that the beam width of the actual directional spectrum of the waves is small. This is likely the case for swell but may be somewhat doubtful for wind waves. For waves or swell near shore the directional spread of the spectra is narrowed by refraction but steepness is enhanced. There is no general way of taking the nonlinear effects associated with large steepness into account for irregular waves, except perhaps by solving the hydrodynamic equations numerically for the particular case at hand. Directional effects of the spectra associated with short-crested waves can be taken into account in the linear theory but in order to be of any use it is required that supplementary information in

---

<sup>4</sup> See for example Lamb (1945). Eqs.(17) and (18) apply at the position where  $\eta$  is measured.

## COASTAL ENGINEERING

regard to water level variations be known. A two-dimensional grid of wave gages could provide the necessary information required in the detailed analysis of short-crested waves. However, in the present analysis we limit our considerations to deductions from  $\eta(t)$  at a single position. It is therefore clear that we are limited to the theory of long-crested waves.

Three quantities of concern in the evaluation of  $F_1$  and  $F_2$  in addition to  $u$  and  $\dot{u}$  are the integrals of  $\dot{u}$ ,  $|z|\dot{u}$  and the gradient of the acceleration at the surface [ see Eq.(11) and (12)]. The last of these quantities is given by

$$\left[ \frac{\partial \dot{u}}{\partial z} \right]_0 = - \int_0^{\infty} M(\omega) \{ \omega^2 k \} \sin [ \omega t - \Theta(\omega) ] d\omega \quad (21)$$

and the integrals in question can be shown to be given by

$$\begin{aligned} I_1 &\equiv \int_{-h_0}^0 \dot{u}(z, t) dz \\ &= - \int_0^{\infty} M(\omega) \left\{ g \frac{\sinh kd - \sinh k(d - h_0)}{\cosh kd} \right\} \sin [ \omega t - \Theta(t) ] d\omega \end{aligned} \quad (22)$$

and

$$\begin{aligned} I_2 &\equiv \int_{-h_0}^0 |z| \dot{u}(z, t) dz \\ &= - \int_0^{\infty} M(\omega) \left\{ g \frac{\cosh kd - kh_0 \sinh k(d - h_0) - \cosh k(d - h_0)}{k \cosh kd} \right\} \\ &\quad \sin [ \omega t - \Theta(t) ] d\omega. \end{aligned} \quad (23)$$

It is possible to utilize Eqs.(17), (18), (21), (22) and (23) directly in the evaluation of the pertinent quantities. However, this is difficult because of the nature of the integrals, but even more important is the fact that for each wave record the two integrals defining  $M(\omega)$  and  $\Theta(\omega)$  must be evaluated. Fortunately a more direct approach exists which bypasses the necessity of the detailed evaluation of the spectral functions, yet is capable of yielding essentially the same results as those indicated implicitly above. However, the foregoing material is an essential step in arriving at the results to follow. The only information required in regard to the wave spectra is an estimate of the effective range of frequencies containing the majority (say 95 percent) of the spectral energy.

CORRELATION OF WATER LEVEL VARIATIONS WITH WAVE  
FORCES ON A VERTICAL PILE FOR NONPERIODIC WAVES

5. NUMERICAL TRANSFORMS OF  $\eta(t)$

For the practical evaluation of the quantities  $u$ ,  $\dot{u}$ ,  $I_1$ ,  $I_2$  or  $\partial \dot{u} / \partial z$  we can make use of one or the other of the following linear transforms of  $\eta(t)$ :

$$G_s [\eta(t)] \equiv a_0 \eta(t) + \sum_{n=1}^N a_n [\eta(t+n\tau) + \eta(t-n\tau)] \quad (24)$$

$$G_a [\eta(t)] \equiv \sum_{n=1}^N b_n [\eta(t+n\tau) - \eta(t-n\tau)] \quad (25)$$

where  $n$  and  $N$  are integers,  $\tau$  is a fixed time interval at which discrete values of  $\eta$  are known and  $a_n$  and  $b_n$  are coefficients which depend upon the type of output  $G(t)$  desired. We will refer to the operation  $G_s [\eta(t)]$  as a symmetrical linear transform of order  $N$ ; while  $G_a [\eta(t)]$  is an anti-symmetrical transform of order  $N$ . It is possible of course to construct an asymmetrical transform by combination of the above two operations but in the present development this general type is not needed. It will be noted that the output depends not only upon the coefficients but is also dependent upon the order and the size of the mesh interval  $\tau$ .

Suppose the input  $\eta(t)$  is given by Eq.(13). The output for operation  $G_s [\eta(t)]$  is readily shown to be

$$G_s(t) \equiv \int_0^\infty R_s(\omega) M(\omega) \cos[\omega t - \Theta(\omega)] d\omega \quad (26)$$

where

$$R_s(\omega) \equiv 2 \left[ \frac{a_0}{2} + \sum_{n=1}^N a_n \cos n\omega\tau \right] \quad (27)$$

On the other hand the output of operation  $G_a [\eta(t)]$  for the same input is

$$G_a(t) = - \int_0^\infty R_a(\omega) M(\omega) \sin[\omega t - \Theta(\omega)] d\omega \quad (28)$$

where

$$R_a(\omega) = 2 \left[ \sum_{n=1}^N b_n \sin n\omega\tau \right] \quad (29)$$

It is therefore evident that the symmetrical numerical transform produces no phase distortion in the output, relative to the input. On the other hand the anti-symmetrical operation alters the phase of each component in the spectrum of the input by  $\pi/2$  radians, so that the output leads the input (if  $b_n$  are positive). In both cases the amplitude spectrum is altered compared with the spectrum of the input, the amount of alteration being specified by the spectral response

## COASTAL ENGINEERING

factors  $R_s$  or  $R_a$ . These response factors are functions of  $\omega$  as determined by the parameters  $\tau$  and  $N$  and the coefficients  $a_n$  or  $b_n$ .

It is evident that the symmetrical transform operation  $G_s[\eta(t)]$  can be useful in the estimation of  $u(z, t)$  provided that the coefficients  $a_n$  can be so chosen that the response factor  $R_s(\omega)$  will approximate the desired response according to Eq.(17). It is also evident that the antisymmetrical operation  $G_a[\eta(t)]$  can be of value in estimating  $\dot{u}(z, t)$  and the other quantities closely associated with the acceleration, provided that the coefficients  $b_n$  can be appropriately chosen so as to produce the desired responses.

Consider the problem of matching  $R_s(\omega)$  with an even function  $R_s'(\omega)$  for  $|\omega| \leq \pi/\tau$ . Since the response factor  $R_s(\omega)$  is expressed as a finite series of cosine functions which are orthogonal in the interval  $-\pi/\tau \leq \omega \leq \pi/\tau$ , it is readily shown that  $R_s(\omega)$  will represent the best approximation of  $R_s'(\omega)$  in the least squares sense for  $|\omega| \leq \pi/\tau$  if

$$a_n = \frac{1}{\pi} \int_0^{\pi} R_s'(\omega) \cos n \phi d\phi, \quad (30)$$

where  $\phi = \omega\tau$  radians and  $n = 0, 1, 2, \dots, N$ . The coefficients  $a_n$  are therefore simply the Fourier coefficients (up to  $n = N$ ) in the cosine expansion of the function  $R_s'(\omega)/2$  for the interval  $-\pi/\tau \leq \omega \leq \pi/\tau$ . It is evident that the accuracy of the approximation of  $R_s'(\omega)$  by  $R_s(\omega)$  for  $|\omega| \leq \pi/\tau$  increases as  $N$  increases. Furthermore, the range of representation of  $R_s'(\omega)$  by  $R_s(\omega)$  is increased by allowing  $\tau$  to decrease. It will be noted of course that the operational response  $R_s(\omega)$ , as given by Eq. (27) is periodic in respect to  $\phi$  with a period equal to  $2\pi$  radians. If  $G_s[\eta(t)]$  is to be an exact predictor of a function whose amplitude spectrum is  $R_s'(\omega)M(\omega)$ , then  $\tau$  should be chosen so that  $M(\omega)$  is negligible for  $|\omega| > \pi/\tau$  and  $N$  should be very large. Furthermore, the range of influence of the numerical operator,  $2N\tau$ , should be large in order that the low frequencies in the spectrum of  $\eta(t)$  are adequately sampled by the numerical operator.

In a similar way  $R_a(\omega)$  as defined by Eq.(29) will approximate an odd function  $R_a'(\omega)$  in the least squares sense for the range  $-\pi/\tau < \omega < \pi/\tau$  provided that

$$b_n = \frac{1}{\pi} \int_0^{\pi} R_a'(\omega) \sin n \phi d\phi \quad (31)$$

where  $n = 1, 2, 3 \dots, N$ . As in the case of the symmetrical transform resp the accuracy of the representation of  $R_a'(\omega)$  by  $R_a(\omega)$ , using the coefficient given by Eq.(31), increases as  $N$  increases, and the resolution in respect to frequency is increased if  $\tau$  is decreased.

CORRELATION OF WATER LEVEL VARIATIONS WITH WAVE  
FORCES ON A VERTICAL PILE FOR NONPERIODIC WAVES  
6. THE VELOCITY AND ACCELERATION PREDICTORS

In the above discussion it was tacitly assumed that no errors exist in the record of  $\eta(t)$ . Actually it is known that the tabulations of  $\eta(t)$  in the present experiment can be in error by  $\pm 0.05$  foot due to rounding off of values to the nearest 0.1 foot. Such errors are random and tend to show up at all frequencies in the energy spectrum for  $\eta(t)$ . The highest detectable frequency in a discrete sequence with time interval  $\tau$  is  $\pi/\tau$ , which corresponds to the limit in range of meaningful response in regard to the transforms  $G_s[\eta(t)]$  or  $G_a[\eta(t)]$ . A high frequency  $\omega > \pi/\tau$  will show up in the discrete sequence as the lower frequency  $\omega' = (2\pi/\tau) - \omega$  and because of the periodic nature of the response functions of the numerical operators, the response for  $\omega$  is equivalent to the response for  $\omega'$ . For this reason we can confine our attention to frequencies less than  $\pi/\tau$ .

If the desired response is such that it approaches zero with increasing  $\omega$  then there is no difficulty encountered in respect to high frequency "noise" created by errors in the input. All that is required is that  $\tau$  is sufficiently small so that the response function is nearly zero for frequencies at or near  $\pi/\tau$ . The response function for  $u(z, t)$ , as given by the quantity in braces in Eq.(17), behaves in the above manner for  $z < 0$ . However, for  $z \geq 0$ , the response function increases without limit as  $\omega$  increases, and it is difficult to simulate this response accurately even over a finite range of frequencies, unless  $N$  is taken very large and  $\tau$  very small. On the other hand, if the response indicated by the hydrodynamical theory is accurately reproduced at high frequencies, then the error "noise" is amplified beyond reasonable bounds and masks the meaningful part of the output. This unwanted amplification of noise can be subdued by filtering out high frequencies, but only at the expense of eliminating some of the meaningful output and thereby introducing error associated with loss of detail. As in many problems of this sort (e.g., communication theory) a compromise in the separation of signal from noise is necessary. The optimum filter would be that for which the combined error in the output has a minimum mean square value. However, the selection of the optimum filter requires a knowledge of the spectrum of the noise as well as that of the signal [see for example, Wiener (1950)].

The procedure employed in the present analysis is much less sophisticated and suffers from being somewhat arbitrary. A cut-off frequency  $\omega_c$  is defined such that the design response is zero for all frequencies in the range  $\omega_c < \omega < \pi/\tau$ . This implies that  $a_n$  and  $b_n$  are to be evaluated from the relations

$$a_n = \frac{1}{\pi} \int_0^{\omega_c \tau} R_s'(\omega) \cos n \phi \, d\phi \quad (32)$$

# COASTAL ENGINEERING

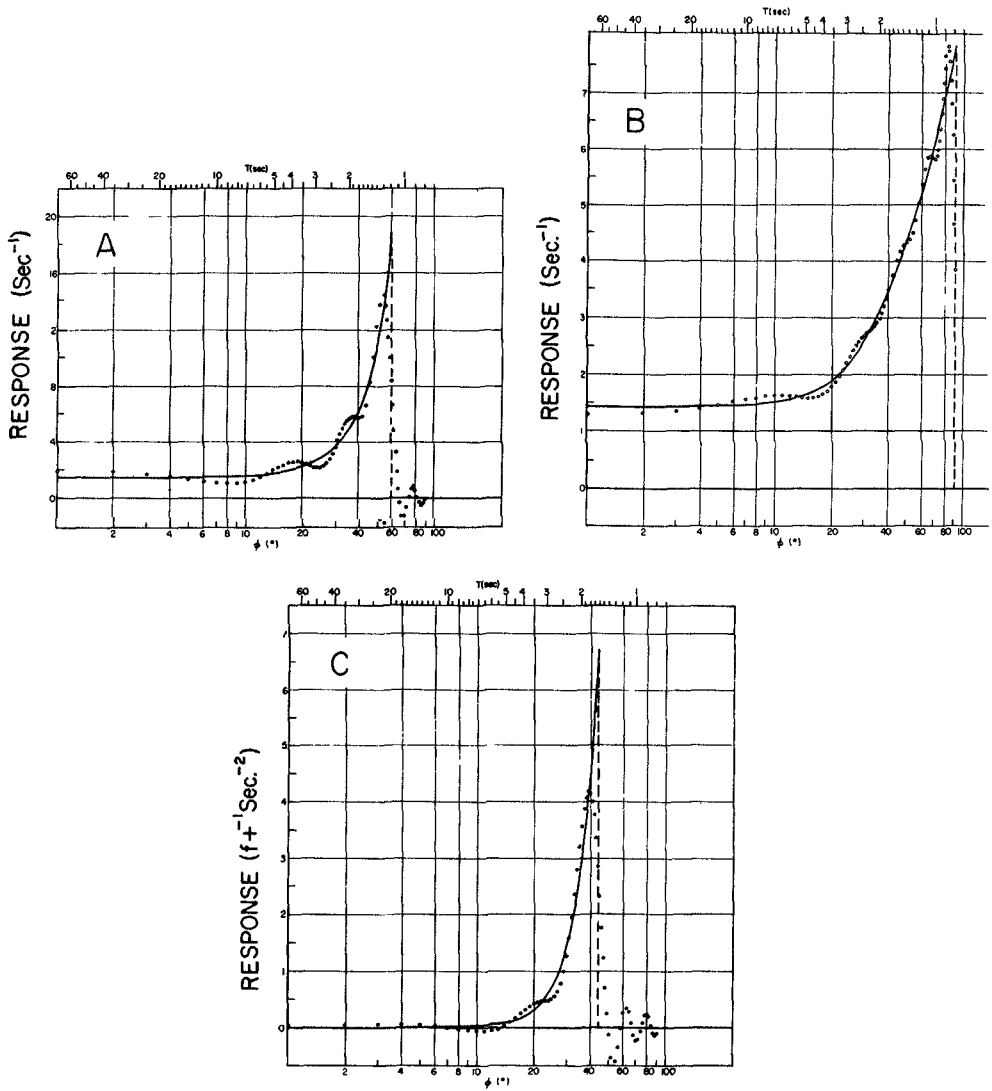


Fig. 5. Response Diagrams for  $u$  at +1.5 feet (A),  $u$  at mean water level (B), and  $\partial u / \partial z$  at mean water level (C). Full curves are from linear wave theory, circled points are from Eq. (36) for velocities and Eq. (3) for graph (C). Design "out-off" shown by vertical dashed line.

CORRELATION OF WATER LEVEL VARIATIONS WITH WAVE  
FORCES ON A VERTICAL PILE FOR NONPERIODIC WAVES

$$b_n = \frac{1}{\pi} \int_0^{\omega_c \tau} R_a'(\omega) \sin n \phi d \phi \quad (33)$$

where it is understood that  $\omega_c < \pi/\tau$ . We stipulate that the selection of  $\omega_c$  for a particular design response in the frequency range  $|\omega| \leq \omega_c$  should satisfy the following conditions:

- (A) The mean square value of the fitted response, as given by (27) or (29), should not deviate from the mean square value of the design response by more than five per cent, for the range  $0 \leq \omega \leq \omega_c$  ;
- (B) The contribution of that portion of the energy spectrum of  $\eta(t)$  for which  $\omega > \omega_c$  should not exceed five per cent of the total spectral energy.

The above conditions also place some restraint upon the selection of  $\tau$  and  $N$ .

Condition (B) can be stated more specifically in the form

$$\int_{\omega_c}^{\infty} M^2(\omega) d\omega < 0.05 \int_0^{\infty} M^2(\omega) d\omega \quad (34)$$

This condition can be tested by comparing the mean square value of  $\eta$  with the mean square value of a filtered counterpart of  $\eta$ , where the filter passes only those frequencies less than  $\omega_c$ . We will return to a further discussion of this in section 7.

In the evaluation of the functions,  $F_1(t)$  and  $F_2(t)$  in Eq.(3) we need  $u(t)$  at seven different levels,  $\dot{u}(t)$  at two levels,  $\partial \dot{u} / \partial z$  at the surface and the integrals  $I_1(t)$  and  $I_2(t)$ , as defined in Eqs.(22) and (23). Consequently seven different transforms of type  $G_s[\eta(t)]$  are required for estimating the seven velocity functions and five different transforms of type  $G_a[\eta(t)]$  are required for the accelerations and the gradient and integrals thereof. The desired responses for these transforms are given by the expressions in braces in Eqs.(17), (18), (21), (22) and (23). These functions are given in column three of Table I. It will be recalled that  $k$  is related to  $\omega$  by Eq.(19); this has been employed in arriving at the particular expressions for the response functions given in Table I. The final values of cut-off period,  $2\pi/\omega_c$ , used in the evaluations of the transform coefficients are indicated in the table. These correspond to  $\phi_c = \omega_c \tau$  as indicated in the last column (expressed in degrees) for  $\tau = 0.2$  second.

The values of  $a_n$  for the seven different velocity predictors and  $b_n$  for the five different acceleration predictors were evaluated numerically by Simpson's rule from Eqs.(32) and (33), using an interval  $\Delta\phi$  of one degree. The values of the pertinent parameters utilized in the computations are as follows:

$\tau = 0.2$ second	$h_0 = 12$ feet
$d = 16$ feet	$\Delta z = 3$ feet

## COASTAL ENGINEERING

The order  $N$  was chosen as 20 for all transforms. The 21 values of  $a_n$  for each of the seven velocity predictors are given in Table II. Each column is labeled according to the  $z$  value to which the coefficients correspond. The units of  $a_n$  are  $\text{sec}^{-1}$ , such that with  $\eta$  in feet the outputs of the  $G_s^{(j)}$  predictors are in feet/sec.

The 20 values of  $b_n$  for each of the five antisymmetrical transforms are given in Table III. The units of each set of  $b_n$  are indicated. It will be noted that the  $b_n$  values for the predictors of  $KI_1$  and  $KI_2$  are given in place of those for  $I_1$  and  $I_2$ , where  $K$  is simply a constant defined by

$$K = \frac{\pi}{4} \frac{w}{g} D^2 \quad (35)$$

which is one of the factors in the equation for  $F_2$ . Taking  $g = 32.2 \text{ ft/sec}^2$ ,  $w = 64 \text{ lbs/cuft}$  and  $D = 8.625 \text{ inches (0.719 feet)}$  leads to the value  $0.806 \text{ lb sec}^2/\text{ft}^2$  for  $K$ .

The response factors for the twelve different predictors, as evaluated by the relations

$$R_s = a_0 + 2 \sum_{n=1}^N a_n \cos n \phi \quad (36)$$

$$R_a = 2 \sum_{n=1}^N b_n \sin n \phi \quad (37)$$

for each degree in the range  $0 < \phi < 90^\circ$ , are indicated by the circled points in Figs. 4, 5 and 6. These responses represent simply the output of the numerical transforms for a simple harmonic input of unit amplitude and frequency  $\omega$ , or period  $T = 2\pi/\omega$ . The scale for  $T$  is related to  $\phi$  by the simple formula

$$T = \frac{360 \tau}{\phi} = \frac{72}{\phi} \quad (38)$$

where  $\phi$  is expressed in degrees and  $\tau = 0.2$  seconds. It will be noted the scales for  $T$  and  $\phi$  are logarithmic. The design response functions are indicated by the full curves in Figs. 4, 5, and 6. The vertical dashed lines indicate the arbitrary cut-off position.

Fig. 4 contains the response functions for velocity at the subsurface levels. The curve for  $z = -15$  feet was added as a matter of interest but was not utilized in the computations of  $F_1$ . The fit of the predictor responses to the desired response is remarkably good owing to the nature of the response curves. The limiting value of response for  $\phi = 0$  (i.e. zero frequency or unlimited  $T$ ) is given by

$$R_s(0) = a_0 + 2 \sum_{n=1}^N a_n \quad (39)$$

# CORRELATION OF WATER LEVEL VARIATIONS WITH WAVE FORCES ON A VERTICAL PILE FOR NONPERIODIC WAVES

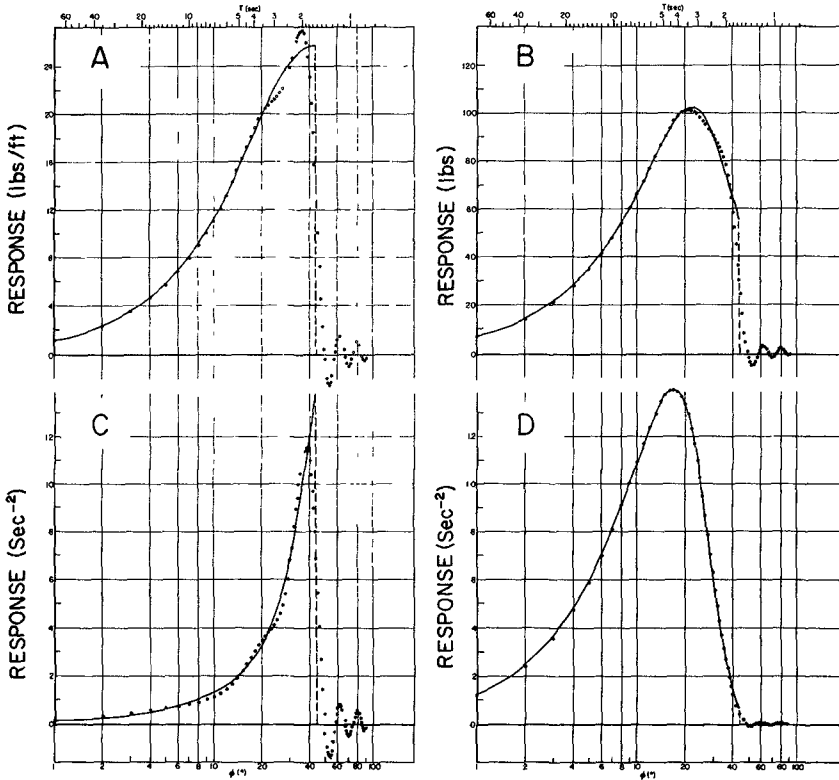


Fig. 6. Response Diagrams for  $KI_1$ (A),  $KI_2$ (B),  $u$  at mean water level (C), and  $u$  at 12 feet below mean water level (D). Full curves are from linear wave theory, circled points from Eq. (37) using  $b_n$  values in Table III. Design "cut-off" shown by vertical dashed line.

TABLE I  
PERTINENT INFORMATION FOR DESIGN OF THE VELOCITY AND ACCELERATION PREDICTORS

Predictor Operation	Design Output	Design Response	$2\pi/\omega_c$	$\phi_c$
$G_s^{(1)}[\eta(t)]$	$u(t)$ at $z = -j\Delta z$	$\omega \frac{\cosh k(d-j\Delta z)}{\sinh kd}$ $(j = -\frac{1}{2}, 0, \frac{1}{2}, 1, 2, 3, 4)$	0.8 sec for $n \geq 0$ 1.2 sec for $n = -\frac{1}{2}$	90° 60°
$G_a^{(1)}[\eta(t)]$	$\dot{u}(t)$ at $z = 0$	$gk$	1.67 sec	44°
$G_a^{(2)}[\eta(t)]$	$\dot{u}(t)$ at $z = -h_0$	$\omega^2 \frac{\cosh k(d-h_0)}{\sinh kd}$	1.67 sec	44°
$G_a^{(3)}[\eta(t)]$	$\partial \dot{u} / \partial z$ at $z = 0$	$\omega^2 k$	1.67 sec	44°
$G_a^{(4)}[\eta(t)]$	$I_1 = \int_{-h}^0 u dz$	$\frac{\omega^2}{k} - g \frac{\sinh k(d-h_0)}{\cosh kd}$	1.67 sec	44°
$G_a^{(5)}[\eta(t)]$	$I_2 = \int_{-h_0}^0  z  u dz$	$\left\{ \frac{g}{k} \left[ 1 - \frac{\cosh k(d-h_0)}{\cosh kd} \right] - gh_0 \frac{\sinh k(d-h_0)}{\cosh kd} \right\}$	1.67 sec	44°

TABLE II  
COEFFICIENTS  $a_n$  FOR VELOCITY PREDICTORS  
(Units of  $a_n$  are  $\text{sec}^{-1}$ )

$\eta$	3(ft)												
	1.5	0	-1.5	-3	-6	-9	-12						
0	1.8495	2.0426	0.7217	0.4162	0.2460	0.1911	0.1674						
1	1.3013	0.9864	0.5134	0.3482	0.2273	0.1820	0.1614						
2	0.0623	-0.7209	0.1029	0.1925	0.1785	0.1570	0.1446						
3	-0.9752	-0.9402	-0.1400	0.0468	0.1168	0.1220	0.1198						
4	-1.1343	0.0638	-0.1187	-0.0276	0.0606	0.0845	0.0913						
5	-0.4531	0.4929	-0.0215	-0.0382	0.0211	0.0510	0.0632						
6	0.4128	-0.0396	0.0011	-0.0236	0.0002	0.0254	0.0387						
7	0.7676	-0.3485	-0.0148	-0.0094	0.0069	0.0087	0.0197						
8	0.4274	0.0338	-0.0004	-0.0004	-0.0066	-0.0004	0.0066						
9	-0.2029	0.2853	0.0206	0.0040	-0.0040	-0.0040	-0.0010						
10	-0.5439	-0.0105	0.0093	0.0042	-0.0016	-0.0046	-0.0045						
11	-0.3499	-0.2238	-0.0085	0.0026	-0.0002	-0.0038	-0.0053						
12	0.1281	0.0129	-0.0008	0.0017	0.0004	-0.0025	-0.0046						
13	0.4255	0.1929	0.0114	0.0016	0.0004	-0.0015	-0.0033						
14	0.2987	-0.0083	0.0023	0.0007	0.0003	-0.0007	-0.0019						
15	-0.0873	-0.1673	-0.0094	-0.0005	0.0002	-0.0002	-0.0008						
16	-0.3466	0.0055	-0.0022	-0.0005	0.0000	0.0001	-0.0001						
17	-0.2591	0.1464	0.0076	-0.0000	-0.0000	0.0003	0.0004						
18	0.0593	-0.0054	0.0008	-0.0003	-0.0000	0.0003	0.0005						
19	0.2900	-0.1319	-0.0076	-0.0007	-0.0000	0.0002	0.0005						
20	0.2265	0.0038	-0.0013	-0.0003	-0.0000	0.0002	-0.0004						

CORRELATION OF WATER LEVEL VARIATIONS WITH WAVE  
FORCES ON A VERTICAL PILE FOR NONPERIODIC WAVES

TABLE III

COEFFICIENTS  $b_n$  FOR ACCELERATION PREDICTORS

$\eta$	Predictor for Units of $b_n$	$\dot{u}_0$ ( $\text{sec}^{-2}$ )	$\dot{u}_{-1/2}$ ( $\text{sec}^{-2}$ )	$\frac{\partial \dot{u}}{\partial z}$ ( $\text{ft}^{-1} \text{sec}^{-2}$ )	$KI_1$ (lbs/ft)	$KI_2$ (lbs)
1		0.6588	0.0579	0.1969	1.9890	7.1693
2		1.0731	0.1057	0.3107	3.3616	12.4422
3		1.0497	0.1355	0.2729	3.6439	14.3793
4		0.7619	0.1450	0.1635	3.1107	13.4307
5		0.2177	0.1349	-0.0237	1.8254	9.8450
6		-0.2990	0.1109	-0.1830	0.4189	5.3314
7		-0.5903	0.0803	-0.2488	-0.6075	1.4142
8		-0.5737	0.0501	-0.2013	-0.9808	-0.9105
9		-0.3070	0.0253	-0.0729	-0.7339	-1.4478
10		0.0519	0.0082	0.0706	-0.1463	-0.7208
11		0.3254	-0.0014	0.1626	0.4139	0.3915
12		0.3991	-0.0055	0.1665	0.6665	1.1023
13		0.2672	-0.0063	0.0909	0.5319	1.0452
14		0.0221	-0.0057	-0.0193	0.1362	0.3535
15		-0.2005	-0.0047	-0.1068	-0.2808	-0.5071
16		-0.2925	-0.0038	-0.1311	-0.5002	-1.0394
17		-0.2230	-0.0027	-0.0870	-0.4318	-0.9823
18		-0.0459	-0.0014	-0.0034	-0.1441	-0.4204
19		0.1363	-0.0001	0.0735	0.1881	0.2998
20		0.2286	0.0009	0.1051	0.3852	0.7815

## COASTAL ENGINEERING

The values of this quantity for each of the velocity predictors are given at the bottom of Table II. The theoretical response at zero frequency (i.e. for very long waves) is simply  $\sqrt{g/d}$  for all levels and has the value  $1.4186 \text{ sec}^{-1}$  for the present case ( $d = 16$  feet). The subsurface velocity predictors give  $R_S(0)$  values well within one per cent of this value. However, the predictors for  $u$  at and above the mean water level are much less accurate, as should be expected from the form of the response functions (Figs. 5A and 5B). However, even for the least accurate of the predictors (that for  $u$  at +1.5 ft elevation) the mean square value of  $R_S$  is less than two per cent different from the mean square value of the design response  $R_S'$  for the interval  $0 \leq \omega \leq \omega_c$ , which is therefore consistent with condition A stipulated earlier.

The response function for  $\partial \dot{u} / \partial z$  at mean water level (Fig. 5C) and  $\ddot{u}$  at mean water level (Fig. 6C) behave in a manner similar to  $u$  at or above the surface, except for one important difference: the response is zero at  $\phi = \omega = 0$ . In fact, this latter condition holds for all five of the antisymmetrical transforms used in the prediction of the acceleration and functions thereof. The response factors for the case of  $KI_1$ ,  $KI_2$ , and  $\dot{u}$  at -12 feet (Figs. 6A, 6B and 6D, respectively) are certainly satisfactory but evidently an improvement could be made by selection of a smaller cut-off period. However, it will be apparent in the discussion which follows that any improvement in response of the acceleration transforms for  $T < 1.6$  seconds will have little influence on the final results in respect to the inertial coefficient. On the other hand the accuracy of the response of the velocity predictors for periods less than 1.6 seconds does affect the evaluation of drag coefficient, and accounts for the selection of the lower cut-off period in the case of those transforms. This is true in spite of the fact that both of the forcing functions  $F_1(t)$  and  $F_2(t)$  are filtered to eliminate all periods less than 1.6 seconds. As discussed earlier, the nonlinear dependence of  $F_1(t)$  on  $u(t)$  implies that the low frequency end of the spectrum of  $F_1(t)$  is partially dependent upon the high frequency end of the spectrum of  $u(t)$ .

### 7. THE VIBRATIONAL FILTER

It was pointed out that the structure and test pile were not free of vibrations. The primary ranges of resonant periods,  $1.1 \pm 0.1$  second and  $0.5 \pm 0.1$  second, were evaluated analytically (Wilson and Reid, 1955) and verified in the experimental records. The effects of these vibrations can be eliminated from the recorded reaction  $R_1(t)$  by employing a symmetrical filter operation of the type

$$F^*(t) \equiv c_0 + 2 \sum_{n=1}^N c_n [F(t + n\tau) + F(t - n\tau)] \quad (40)$$

where  $F(t)$  is the particular time sequence to be filtered [e.g.  $R_1(t)$ ]. The

# CORRELATION OF WATER LEVEL VARIATIONS WITH WAVE FORCES ON A VERTICAL PILE FOR NONPERIODIC WAVES

desired characteristics of this filter are: unit response for  $T > T_c$  and zero response for  $T < T_c$  where  $T_c$  is a nominal cut-off period which will assure the elimination of all vibrational effects. The operation (40), of course, is free of any phase distortion for  $T > T_c$ . The above response characteristics are approximated by taking

$$c_n = \frac{1}{\pi} \int_0^{2\pi\tau/T_c} \cos n\phi \, d\phi \quad (41)$$

which yields

$$c_0 = \frac{2\tau}{T_c} \quad (42)$$

and

$$c_n = \frac{1}{n\pi} \sin \frac{2\pi n\tau}{T_c} \quad (43)$$

for  $n = 1, 2, \dots, N$ . The amplitude response factor of the filter for simple harmonic input is

$$R_s = c_0 + 2 \sum_{n=1}^N c_n \cos n\phi \quad (44)$$

A continuous graph of this function for  $T_c = 1.6$  seconds and  $N = 20$  is shown in Fig. 7. It can be seen that this response assures almost complete suppression of the vibrational periods.

This filter has two important functions: (a) application to the sequences of  $R_1(t)$ ,  $F_1(t)$ , and  $F_2(t)$  to assure suppression of a common band of high frequencies in all three records and (b) application to the sequence  $\eta(t)$  in order to gain some information in regard to the spectrum of this sequence.

The primary function of the filter of course is the suppression of vibrations in the  $R_1(t)$  sequence. If the filter had perfect unit response for  $T > 1.6$  seconds and if the sequences  $F_1(t)$  and  $F_2(t)$  contained no spectral energy for  $T < 1.6$  seconds then there would be no need of filtering these time series since the output would be the same as the input. However, the filter is not perfect; there is some amplitude distortion for  $T > 1.6$  seconds as is evident in Fig. 7. Furthermore, the sequence  $F_1(t)$  will definitely contain spectral energy for  $T < 1.6$  seconds, as provided by the relatively small cut-off periods in the design of the velocity predictors. In addition, high as well as low frequencies are generated by the nonlinear transformation leading to  $F_1(t)$ . This is the case to a lesser degree in regard to  $F_2(t)$ . In view of these considerations it is apparent that each of the functions  $R_1(t)$ ,  $F_1(t)$ ,  $F_2(t)$  should be subjected to the same filtering operation if they are to be analysed on a comparable basis.

## COASTAL ENGINEERING

Figure 8 illustrates the degree of smoothing accomplished by the above filter when applied to a record of water level variations. Here  $\eta(t)$  is the original record and  $\eta^*(t)$  is the filtered output. It will be noted that an interval of  $N\tau$  (4 seconds) is lost at each end of the finite record in the filter process. From these two sequences it is possible to ascertain the relative amount of spectral energy of water level variations for all periods less than the cut-off period of 1.6 seconds. This relative spectral energy is given by

$$1 - \frac{\overline{(\eta^*)^2}}{\overline{\eta^2}} \quad (45)$$

where the averages are taken over the same time interval for both sequences. The value of this quantity was found to be 0.038 based upon a total of 280 seconds of filtered record (sampled from all runs). Thus the net effect of all periods less than 1.6 seconds in the spectrum of  $\eta(t)$  contributes less than four per cent to the total spectral energy, for the data utilized in the present study. The cut-off period for the acceleration predictors was taken as 1.67 seconds which is only slightly greater than the cut-off for the vibrational filter. It therefore appears that condition B of section 6, as expressed by the inequality (34), is satisfied for the mean conditions.

### 8. ANALYSIS OF THE DATA

The application of the numerical transform operations  $G_s[\eta(t)]$  and  $G_a[\eta(t)]$  is illustrated schematically in Figs. 9A and 9B; here the input, weighting factors  $a_n$  or  $b_n$ , and the output are shown diagrammatically. The output curve is generated by shifting the product and summing operation progressively along the  $t$  axis [see Eqs.(24) and (25)].

As an illustration of the type of vertical distribution of currents obtained from the wave records, some sample results of the velocity transforms for a particular run are shown in Fig. 10A. The distributions of current at five different times are shown, each curve terminating at an elevation dependent upon the instantaneous value of  $\eta$ . In each case the velocities at  $z = 0$  and  $z = 1.5$  ft were used in estimating the shape of the curve near the surface. The appropriate portion of the water level record from which the velocity distributions were obtained is shown in Fig. 10B.

The sequence of evaluation of  $F_1(t)$  and  $F_2(t)$  and finally  $C_D$  and  $C_M$  by use of the regression formula (3) is indicated in the schematic flow diagram of Fig. 11. The entire program of computations was carried out by an electronic digital computer. The seven transforms of type (24) and five transforms of type (25) with coefficients as stipulated in Tables II and III were utilized in the evaluation of the velocities  $u(z, t)$  and the acceleration functions respectively. The mean current  $U(z)$  was estimated from measurements of the surface drift (Reid, 1956). The mean surface current ranged

# CORRELATION OF WATER LEVEL VARIATIONS WITH WAVE FORCES ON A VERTICAL PILE FOR NONPERIODIC WAVES

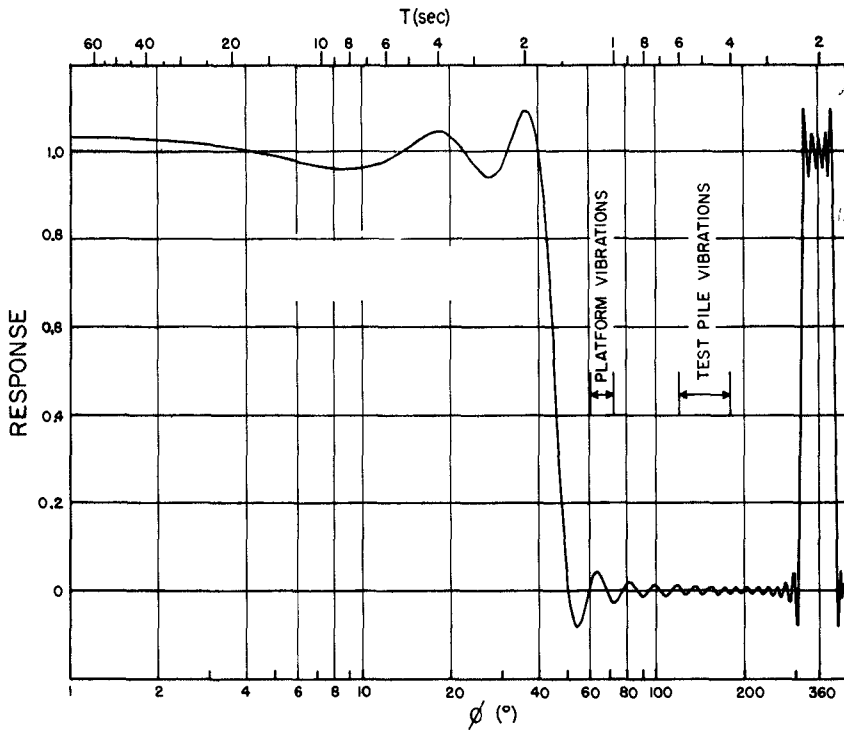


Fig. 7. Response diagram for vibration filter with nominal "cut-off" at 1.6 seconds. Based upon Eqs.(42), (43) and (44) with  $\tau = 0.2$  seconds,  $N = 20$ .

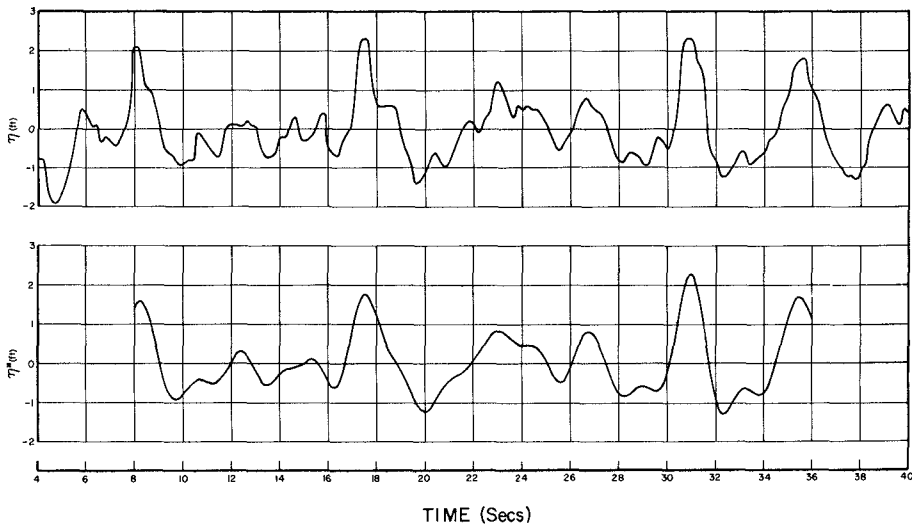


Fig. 8. Illustration of original and filtered sequence of water level variations (Run 2);  $\eta^*(t)$  is the output of filter operation (40) with input  $\eta(t)$  and spectral response as depicted in Fig. 7.

# COASTAL ENGINEERING

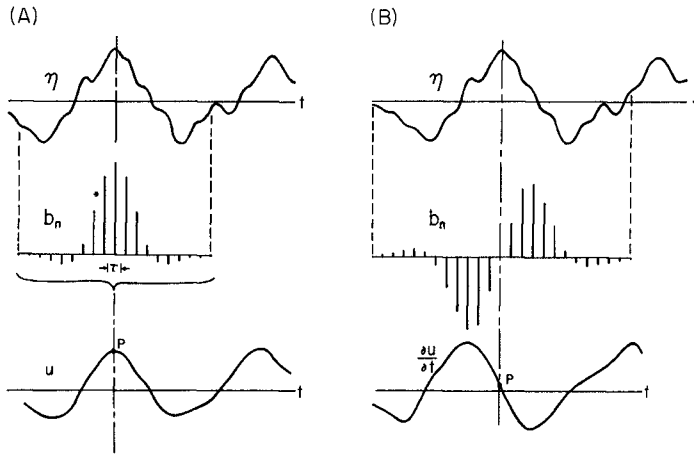


Fig. 9. Schematic of numerical transform operation for symmetrical (A) and antisymmetrical (B) transforms, showing input, weighting coefficients and output.

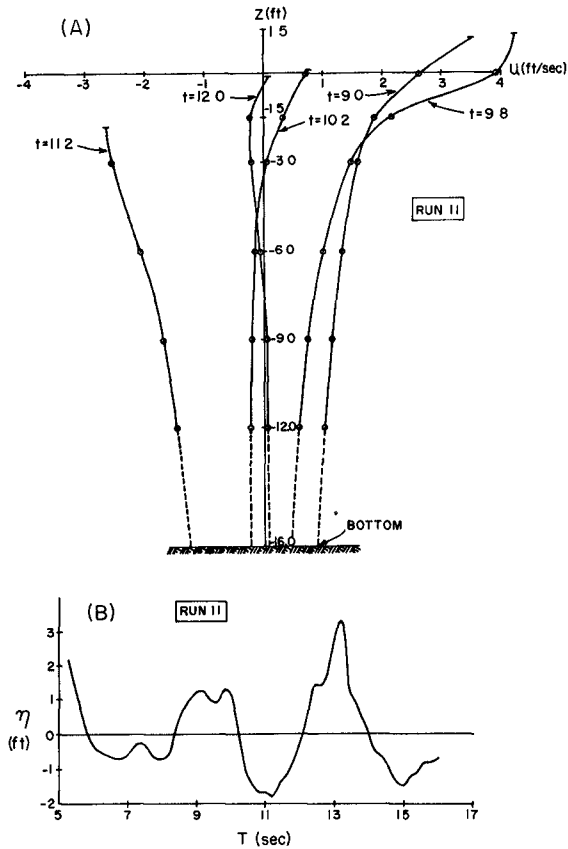


Fig. 10. Illustration of the vertical distribution of velocity  $u$  for five different times (A) as deduced by numerical transformation of the water level sequence (B) for run 11.

CORRELATION OF WATER LEVEL VARIATIONS WITH WAVE FORCES ON A VERTICAL PILE FOR NONPERIODIC WAVES

TABLE IV  
SAMPLE LISTINGS OF ORIGINAL AND COMPUTED SEQUENCES FOR RUN 11

Run	t (sec)	$u(1,5)$ (ft/sec)	$u(0)$ (ft/sec)	$u(-1,5)$ (ft/sec)	$u(-3)$ (ft/sec)	$u(-6)$ (ft/sec)	$u(-9)$ (ft/sec)	$u(-12)$ (ft/sec)	$\eta$ (ft)	$F_1$ (lbs)	$F_2$ (lbs)	$F_3$ (lbs)	$F_4$ (lbs)	$\gamma^*$ (ft)	$R_1$ (lbs)	$R_2$ (lbs)	$R_3$ (lbs)	$R_4$ (lbs)	
11	14.8	2.668	2.351	2.140	1.887	1.573	1.353	1.212	1.4	30.1	11.4	29.0	1.20	13.2	56.1				
11	15.0	4.379	2.444	2.162	1.925	1.659	1.482	1.366	1.5	36.8	3.7	72.0	1.23	7.0	7.0				48.6
11	15.2	4.445	2.292	1.919	1.797	1.627	1.503	1.421	1.2	35.5	2.6	58.0	1.24	15.8	1.1				39.2
11	15.4	2.822	1.231	1.520	1.567	1.506	1.439	1.393	1.1	29.1	8.7	14.0	1.23	31.7	6.1				26.6
11	15.6	9.93	3.21	1.188	1.315	1.326	1.311	1.300	0.8	22.2	14.6	0.0	1.15	43.9	14.7				10.0
11	15.8	2.41	1.037	1.037	1.082	1.117	1.146	1.162	0.9	16.0	19.0	38.0	0.96	42.8	22.2				8.1
11	16.0	1.056	1.444	0.93	0.855	0.902	0.962	0.995	0.7	11.0	21.0	5.0	0.69	25.9	23.7				31.8
11	16.2	2.104	1.281	0.675	0.612	0.700	0.775	0.810	0.6	6.8	19.6	10.0	0.58	1.0	23.8				31.8
11	16.4	1.789	0.843	0.26	0.378	0.526	0.590	0.609	0.2	3.8	18.6	38.0	0.12	20.2	18.8				32.1
11	16.6	2.519	4.3	4.03	4.21	4.81	4.93	4.91	0	4.1	8.5	19.0	0.00	26.2	8.4				27.0
11	17.0	2.883	5.11	0.271	0.191	0.254	0.254	0.201	0	1.1	7.0	29.0	0.02	16.0	8.6				21.8
11	17.2	0.842	1.275	0.571	0.268	0.108	0.095	0.123	0.1	5.0	7.2	14.0	0.15	9.1	8.6				33.2
11	17.4	1.889	1.889	0.560	0.092	0.439	0.869	0.859	0.2	2.2	17.2	14.0	0.28	26.5	18.4				34.0
11	17.6	3.058	0.883	0.113	0.092	0.439	0.869	0.859	0.2	2.2	17.2	14.0	0.28	26.5	18.4				34.0
11	17.8	1.713	0.199	0.819	0.212	1.421	1.453	1.407	0.1	2.8	32.2	62.0	0.09	9.1	51.7				19.3
11	18.0	1.847	1.448	2.180	2.229	2.003	1.845	1.507	1.4	64.5	60.8	106.0	1.84	132.6	52.1				110.0
11	18.2	5.983	3.866	3.697	3.170	2.814	1.992	1.764	2.1	151.4	43.4	101.0	2.53	221.7	2.2				74.5
11	18.4	8.267	6.770	4.758	3.680	2.957	2.014	1.740	2.8	312.6	3.9	91.0	2.53	221.7	2.2				101.7
11	18.6	8.267	4.668	3.487	2.353	1.823	1.423	1.560	2.9	333.6	47.3	48.0	2.36	213.7	37.5				34.6
11	18.8	5.214	4.655	3.254	2.569	1.812	1.431	1.236	1.8	122.4	78.4	5.0	1.74	168.7	65.9				9.9
11	19.0	0.665	0.252	1.124	1.193	1.031	0.831	0.608	0.7	17.1	83.7	86.0	0.82	100.5	80.2				49.4
11	19.2	3.544	2.446	0.806	0.228	0.169	0.288	0.330	0.5	1.2	70.1	86.0	0.16	29.3	77.6				77.7
11	19.4	5.879	2.741	2.020	1.349	0.610	0.284	0.134	0.2	10.1	54.3	53.0	0.97	25.6	60.6				90.5
11	19.6	5.743	2.506	2.565	2.006	1.182	0.747	0.526	1.4	25.6	32.9	115.0	1.86	35.3	35.3				70.2
11	19.8	3.844	3.074	2.651	2.195	1.485	1.047	0.803	1.5	28.3	12.2	58.0	1.58	53.5	9.1				42.6
11	20.0	1.499	3.313	2.328	2.006	1.526	1.164	0.943	1.4	25.0	16.1	29.0	1.40	35.6	11.8				8.6
11	20.2	0.74	1.896	1.645	1.578	1.355	1.113	0.947	1.1	20.8	20.7	29.0	1.07	13.1	24.7				25.8
11	20.4	0.355	0.888	0.888	1.070	1.047	0.930	0.837	0.7	12.1	29.5	58.0	0.70	3.4	29.6				57.1
11	20.6	5.222	0.510	4.03	0.604	0.671	0.666	0.648	1.1	4.4	32.3	34.0	0.36	9.1	28.9				78.9
11	20.8	1.488	0.297	0.209	0.286	0.374	0.374	0.425	0.3	1.4	28.4	62.0	0.08	5.9	20.5				87.7
11	21.0	1.512	0.981	0.16	0.183	0.061	0.104	0.209	0.1	3.2	18.5	70.0	0.15	0	14.6				81.3
11	21.2	0.92	0.548	0.548	0.577	0.330	0.103	0.036	0.2	3.2	18.5	53.0	0.35	2.8	7.2				60.2
11	21.4	1.898	1.931	1.227	0.894	0.472	0.219	0.069	0.7	14.7	6.8	91.0	0.49	1.3	1.9				30.3
11	21.6	3.408	3.128	1.827	0.987	0.481	0.232	0.100	0.9	28.9	6.0	29.0	0.84	9.5	16.2				11.7
11	21.8	3.238	2.280	1.223	0.749	0.352	0.152	0.063	0.6	15.2	15.4	100.0	0.85	16.2	11.7				23.5
11	22.0	1.333	0.136	0.349	0.230	0.070	0.006	0.021	0.2	1.3	23.0	19.0	0.21	18.7	19.6				51.0
11	22.2	1.233	1.488	0.603	0.390	0.236	0.066	0.021	0.2	1.3	23.0	19.0	0.21	18.7	19.6				21.2
11	22.4	3.019	1.873	1.290	0.907	0.503	0.309	0.210	0.7	4.1	18.3	24.0	0.77	3.8	19.3				2.9
11	22.6	1.336	1.925	1.590	1.171	0.653	0.389	0.254	0.8	6.8	8.4	5.0	0.73	4.9	34.5				63.2
11	22.8	1.610	2.172	1.514	1.132	0.647	0.378	0.236	0.8	6.0	4.7	58.0	0.69	6.3	19.2				80.7
11	23.0	0.425	1.856	1.071	0.822	0.483	0.270	0.154	0.6	3.2	18.2	58.0	0.74	2.0	2.4				82.4
11	23.2	1.611	0.435	0.372	0.339	0.199	0.085	0.019	0.2	2.2	34.9	77.0	0.30	5.3	32.7				69.5
11	23.4	1.404	1.026	0.324	0.194	0.145	0.141	0.143	0.2	3.2	34.9	77.0	0.30	5.3	32.7				45.4
11	23.6	0.430	1.225	0.677	0.481	0.364	0.202	0.123	0.6	8.7	31.3	72.0	0.56	14.0	27.8				16.5
11	23.8	0.050	0.762	1.163	1.054	0.743	0.537	0.323	0.6	12.1	17.9	29.0	0.86	20.8	15.9				11.1
11	24.0	0.918	1.185	1.486	1.285	0.880	0.623	0.479	0.7	18.5	1.2	34.0	0.96	23.3	4.4				33.6
11	24.2	2.372	2.502	1.692	1.311	0.863	0.600	0.451	1.0	29.0	16.0	0.0	0.66	21.2	14.7				47.4
11	24.4	3.105	2.906	1.498	1.079	0.688	0.466	0.338	1.1	31.2	28.3	19.0	0.26	8.9	32.2				57.7
11	24.6	2.090	1.244	0.800	0.606	0.380	0.238	0.150	0.2	6.6	30.8	77.0	0.26	8.9	32.2				50.8
11	24.8	0.356	0.935	1.02	0.009	0.054	0.049	0.089	0	0	31.3	53.0	0.08	2.9	57.7				29.2
11	25.0	2.897	1.527	0.811	0.579	0.419	0.368	0.347	0.5	2.7	28.6	29.0	0.38	1.6					

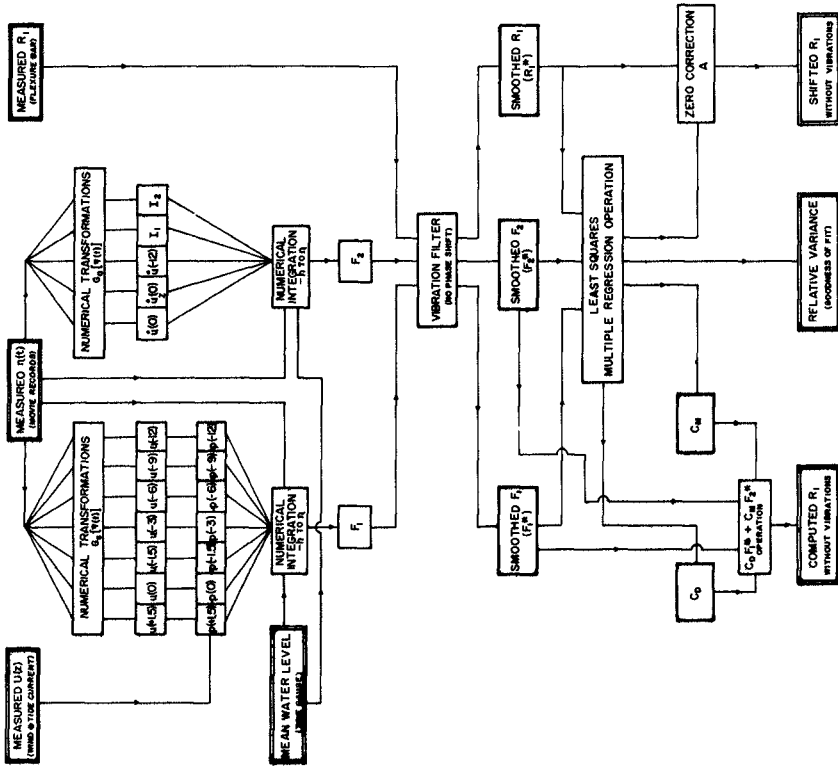


Fig. 11. Schematic flow diagram in the numerical analysis of the water level and reaction data, lead-  
 ing to the determination of the mean and in-phase coefficients

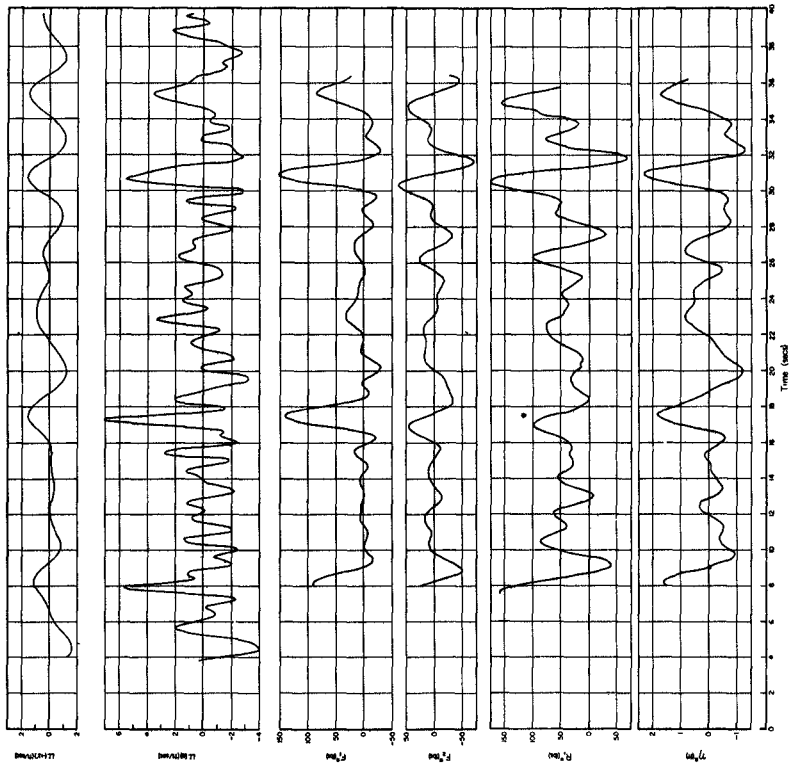


Fig. 12. Samples of simultaneous serial sequences of  $u$  at -12 feet,  $u$  at mean water level,  $F_1^*$ ,  $F_2^*$ ,  $R_1^*$ , and  $\eta^*$  as computed from the basic sequences  $R_1(t)$  and  $\eta^*(t)$

# CORRELATION OF WATER LEVEL VARIATIONS WITH WAVE

## FORCES ON A VERTICAL PILE FOR NONPERIODIC WAVES

from about 0.5 to 0.7 ft/sec, with much smaller values at subsurface depths. In contrast with the steady current, the values of  $u$  at the surface cover a range from about -5 to +10 ft/sec, considering all runs. For the most part, the effect of the steady component of current constituted a second order correction in respect to the evaluation of  $p$  as defined by Eq.(7) .

The time sequences of  $p_1$  ,  $\dot{u}$  ,  $\partial \dot{u} / \partial z$  ,  $I_1$  , and  $I_2$  were utilized together with  $\eta(t)$  and  $h$  (as inferred from the tide gage) in the evaluation of  $F_1(t)$  and  $F_2(t)$  using definitions (4) and (5) together with the auxiliary formulas (8) to (12). The values of  $h$  ranged from 11.1 to 12.0 feet for the three different series of runs. The values of  $L$  and  $b$  in Eqs.(4) and (5) were taken as 30.8 feet and 9.0 feet respectively.

The measured sequence  $R_1(t)$  and the computed sequences  $F_1(t)$  and  $F_2(t)$  for each run were filtered to eliminate all periods in the vibrational range. The outputs of the filter operation are designated as  $R_1^*(t)$ ,  $F_1^*(t)$  and  $F_2^*(t)$  respectively. A sample plot of these sequences for one run is given in Fig. 12. These are compared with a filtered version of the water level sequence from which  $F_1^*(t)$   $F_2^*(t)$  were derived. As a matter of interest, the sequences of  $u$  at mean water level and -12 feet are also included in the figure. A sample listing of the calculations of  $u$  (at all seven levels),  $\eta$ ,  $F_1$ ,  $F_2$ ,  $R_1$ , and the filtered sequences  $\eta^*$ ,  $F_1^*$ ,  $F_2^*$ ,  $R_1^*$  is given in Table IV.

As stipulated earlier, Eq.(3) is valid only in the absence of vibrations or if the functions involved are interpreted as the sequences from which vibrations have been effaced. In addition, it was stipulated that the true zero reference in the measurements of  $R_1$  could not be ascertained with certainty. Consequently, allowance for this should be made by incorporating a constant correction term  $A$  such that  $R_1 - A$  is the true reaction. Because of the possibility of zero drift in the measuring equipment, we must expect differences in  $A$  from one run to another. Thus there are really three coefficients  $A$ ,  $C_D$  and  $C_M$  which are to be evaluated by least squares multiple regression procedure for each run.

With the above changes, the appropriate regression equation becomes

$$R_1'(t) = C_D F_1^*(t) + C_M F_2^*(t) \quad (46)$$

which is to be fitted to the sequence  $R_1^*(t) - A$  . Here  $R_1'(t)$  is the predicted value of filtered reaction for a particular set of constants  $A$ ,  $C_D$ ,  $C_M$  . We seek those values of  $A$ ,  $C_D$ , and  $C_M$  which make the quantity

$$S_e^2 \equiv \frac{1}{P} \sum_{n=1}^P [A + C_D F_1^*(t_n) + C_M F_2^*(t_n) - R_1^*(t_n)]^2 \quad (47)$$

a minimum, where  $P$  is the total number of points in each sequence. The

TABLE V  
SUMMARY OF RESULTS OF WAVE FORCE ANALYSIS

Sun Oil Co. Pier, Caplen, Texas,  $d = 16$  feet,  $D = 8.625$  inches.

Supplementary Data	Run	P total points	$Z^2$ (ft)	$N_T$ $10^5$	$S_e$ (lbs)	$S_R$ (lbs)	$C_D$	$C_M$	$r$
<u>Series I.</u>									
Date: Feb. 27, 1954									
Time: 1704-1708 h CST									
Wind: 21 mph SW									
$U_0 = 0.5$ ft/sec									
$h = 12.0$ ft									
$H_S = 2.3$ ft, $T_m = 3.5$ sec									
	1	89	0.80	0.60	25	46	0.73	1.41	0.84
	2	139	0.81	0.61	19	45	0.53	1.39	0.90
	3	149	0.69	0.52	18	49	0.32	1.96	0.93
<u>Series II.</u>									
Date: May 11, 1954									
Time: 1630-1642 h CST									
Wind: 18 mph SE									
$U_0 = 0.5$ ft/sec									
$h = 11.4$ ft									
$H_S = 2.6$ ft, $T_m = 4.3$ sec									
	5	65	0.63	0.48	12	23	0.27	1.63	0.93
	7	57	1.03	0.76	23	56	0.63	1.60	0.91
	8	71	0.76	0.56	14	45	0.82	1.92	0.95
	9	88	1.01	0.86	18	54	0.42	1.72	0.94
	10	92	0.78	0.58	17	43	0.88	1.45	0.92
	11	114	1.07	0.78	22	62	0.54	1.45	0.94
<u>Series III.</u>									
Date: May 11, 1954									
Time: 1852-1906 h									
Wind: 22 mph SE									
$U_0 = 0.7$ ft/sec									
$h = 11.1$ ft									
$H_S = 3.3$ ft, $T_m = 4.8$ sec									
	12	71	1.24	0.91	32	63	0.88	0.41	0.86
	13	55	1.32	0.97	25	71	0.80	0.80	0.94
	14	84	1.62	1.18	35	86	0.33	1.37	0.91
	15	95	0.74	0.56	14	29	0.37	1.16	0.87
	16	95	0.93	0.70	20	51	0.33	1.70	0.92
	17	82	1.09	0.81	15	56	0.44	1.57	0.97
	18	46	1.01	0.76	11	47	0.44	1.36	0.97
	Total	1392		Weighted averages <sup>2</sup>	21	58	0.53	1.47	
									Overall correlation = 0.93

1 The wind speed and directions are averages for preceding 6 hour period.  
 2 The overall values of  $S_e$  and  $S_R$  are root mean square values weighted according to P.  
 The overall  $C_M$  and  $C_D$  are averages weighted according to P

CORRELATION OF WATER LEVEL VARIATIONS WITH WAVE  
FORCES ON A VERTICAL PILE FOR NONPERIODIC WAVES

quantity  $S_e$  represents the standard deviation of the measured reaction from the predicted or fitted reaction. The requirement of minimum  $S_e$  leads to three equations from which the three coefficients are derived. The resulting solutions are symbolically:

$$C_D = \frac{1}{Q} \left\{ [R_1^*, F_1^*] [F_2^*, F_2^*] - [R_1^*, F_2^*] [F_1^*, F_2^*] \right\} \quad (48)$$

$$C_M = \frac{1}{Q} \left\{ [R_1^*, F_2^*] [F_1^*, F_1^*] - [R_1^*, F_1^*] [F_1^*, F_2^*] \right\} \quad (49)$$

where

$$Q = [F_1^*, F_1^*] [F_2^*, F_2^*] - [F_1^*, F_2^*]^2 \quad (50)$$

and

$$A = \overline{R_1^*} - C_D \overline{F_1^*} - C_M \overline{F_2^*} \quad (51)$$

In the above equations the following special notation is employed for the covariance of any pair of sequences  $f_1(t)$  and  $f_2(t)$  having non-zero means:

$$[f_1, f_2] \equiv \overline{f_1 f_2} - \overline{f_1} \overline{f_2} \quad (52)$$

where the bar indicates an average taken over a total of  $P$  discrete values. It is of interest to note that in the special case where  $F_1^*$  and  $F_2^*$  possess zero mean value and zero covariance then the above relations reduce to the remarkably simple form:

$$C_D = \frac{\overline{R_1^* F_1^*}}{\overline{(F_1^*)^2}} \quad (53)$$

$$C_M = \frac{\overline{R_1^* F_2^*}}{\overline{(F_2^*)^2}} \quad (54)$$

$$A = \overline{R_1^*} \quad (55)$$

These relations would be directly applicable to simple harmonic waves such as are obtained approximately in the laboratory studies, assuming that  $U$  is zero.

In the complex records analysed it was found that the above simplification was not applicable since the covariance  $[F_1^*, F_2^*]$  was small but not negligible and also the mean value of  $F_1^*$  was finite. Consequently the general relations (48) through (52) were employed in the numerical evaluation of the coefficients. The results of the calculations for each run are summarized in Table V. Supplementary information for each series of runs is included.

## COASTAL ENGINEERING

The parameter  $S_R^2$  is the variance of  $R_1^*$  from its mean value, i.e.

$$S_R^2 = \overline{(R_1^*)^2} - [\overline{R_1^*}]^2 \quad (56)$$

and  $r$  is the correlation coefficient, characterizing the goodness of fit of the functions  $F_1^*(t)$  and  $F_2^*(t)$  to  $R_1^*(t)$ . It is defined by

$$r \equiv \sqrt{1 - \frac{S_e^2}{S_R^2}} \quad (57)$$

perfect correlation being unity.

The quantity  $N_R$  is a root mean square value of the Reynolds number defined by

$$N_R = \frac{D v_R}{\gamma} \quad (58)$$

$\gamma$  being the kinematic viscosity of water (taken as  $1 \times 10^{-5}$  ft<sup>2</sup>/sec) and  $v_R$  is the root mean square value of the total current (averaged over the depth and the duration of the run). Note that all values of  $N_R$  given in the table are to be multiplied by  $10^5$ .

The quantity  $H_s$  given with the supplementary data is an estimate of significant wave height as computed from the formula

$$H_s = 2\sqrt{2} \overline{\eta^2} \quad (59)$$

which follows from the analysis by Longuet-Higgins (1952, p.254). The value of  $\overline{\eta^2}$  in this relation is the mean for the particular series of runs. The quantity  $T_m$  is a mean "period" evaluated from the filtered sequence  $\eta^*(t)$ . It is defined as twice the mean time interval between successive zero values of  $\eta^*$ , and is closely related to the significant period of the waves. Series III has the largest significant wave height and largest mean period of the three series. This series followed about two and one-half hours after series II, during which time the wind was steadily gaining in speed out of the southeast. In the series I data the mean wind speed was nearly the same as for series III, but the wind was from the southwest and hence more nearly parallel with the shore line.

It can be shown from the Eq.(47) to (52) that the variance of  $R_1^*$  can be expressed in the form

$$S_R^2 = [R_1^*, F_1^*] C_D + [R_1^*, F_2^*] C_M + S_e^2 \quad (60)$$

where the symbolic covariance notation (52) is employed on the right. This

CORRELATION OF WATER LEVEL VARIATIONS WITH WAVE FORCES ON A VERTICAL PILE FOR NONPERIODIC WAVES

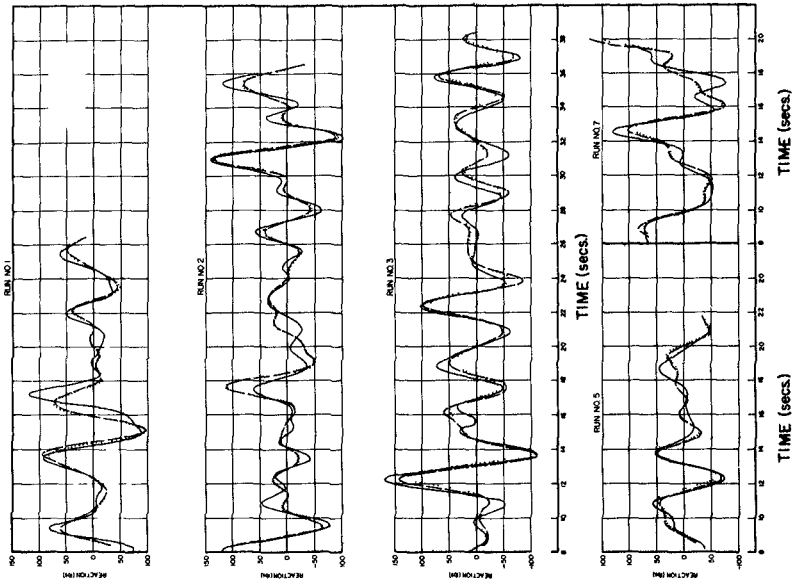


Fig. 13. Graphs of  $R_1^* - A$  (full curves), Regression Function  $R_1'$  (dashed curves), and Predicted Reaction  $R_1''$  (dotted curves) for runs 1, 2, 3, 5, and 7. The dashed curves are based upon the best fit  $C_D$  and  $C_M$  values for the individual runs. The dotted curve is based upon the overall mean values of  $C_D$  and  $C_M$  (0.53 and 1.47 respectively).

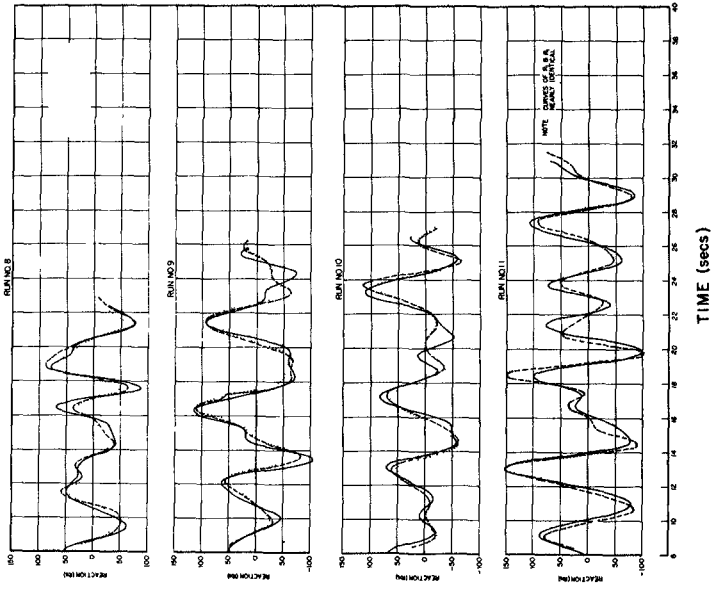


Fig. 14. Graphs of  $R_1^* - A$  (full curves), Regression Function  $R_1'$  (dashed curves) and Predicted Reaction  $R_1''$  (dotted curves) for runs 8, 9, 10, and 11.

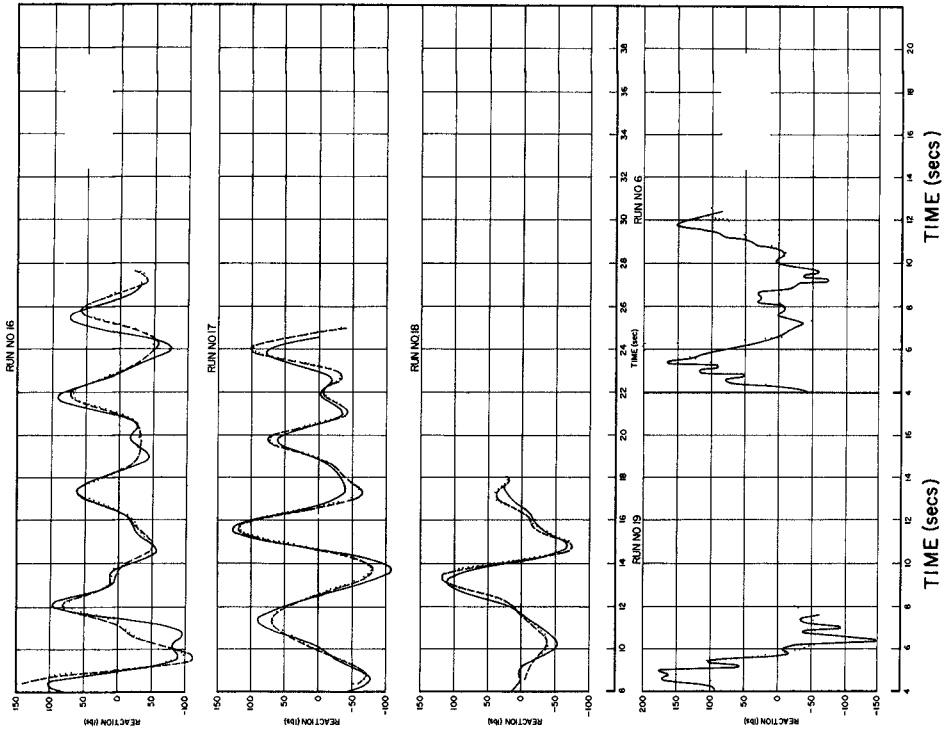


Fig. 16. Graphs of  $R_1^* - A$  (full curves), Regression Function  $R_1^*$  (dashed curves), and Predicted Reaction

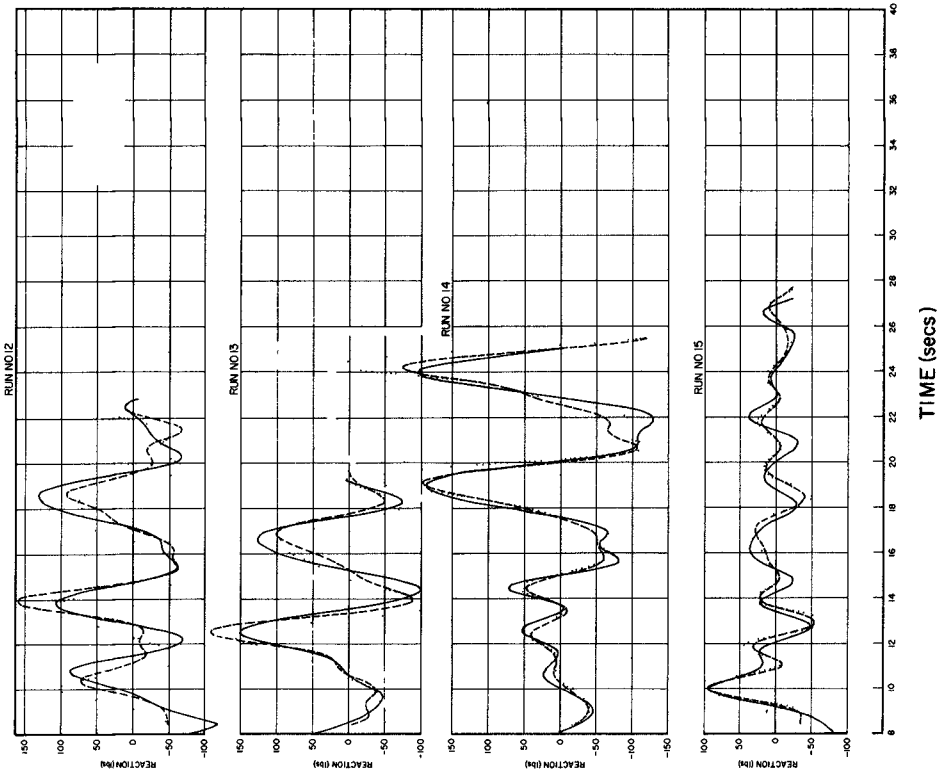


Fig. 15. Graphs of  $R_1^* - A$  (full curves), Regression Function  $R_1^*$  (dashed curves), and Predicted Reaction

# CORRELATION OF WATER LEVEL VARIATIONS WITH WAVE FORCES ON A VERTICAL PILE FOR NONPERIODIC WAVES

relation is useful in the interpretation of the spectral composition of  $R_1^*$ . The sum of the first and second terms on the right represent that part of the total spectral energy of the  $R_1^*$  sequence which is accounted for by the hydrodynamic forces associated with the waves, while the last term is the unaccountable part. The fractional contributions to the energy spectrum of  $R_1^*$  by drag force and inertial force can be evaluated separately from the expressions

$$\frac{[R_1^*, F_1^*] C_D}{S_R^2} \quad \text{and} \quad \frac{[R_1^*, F_2^*] C_M}{S_R^2} \quad (61)$$

respectively.

The overall root mean square values of  $S_e$  and  $S_R$  and the mean values of  $C_D$  and  $C_M$  (all weighted according to the number of points in each run) are indicated in Table V. The overall correlation coefficient of 0.93 was evaluated from (57) using the weighted mean square values of  $S_e$  and  $S_R$ . The set of  $C_D$  values possess a standard deviation of 0.20 from the mean value 0.53, and the set of  $C_M$  values have a standard deviation of 0.36 from the mean value 1.47. The weighted mean values of  $[R_1^*, F_1^*] C_D$  and  $[R_1^*, F_2^*] C_M$  indicate that the drag force contributes about 27 per cent to the variance of  $R_1^*$  while the inertial force contributes about 60 per cent, based upon all runs.<sup>5</sup> The remaining 13 per cent, corresponding to  $S_e^2/S_R^2$  (or  $1 - r^2$ ), is unaccountable insofar as the present hypothesis in regard to the nature of the fluid forces and field of motion is concerned. The fact that the inertial force contribution is of greater importance in the present tests is not surprising in view of the rather small mean "periods" of the waves. It is evident that a proportionately greater degree of reliability exists in respect to the estimates of  $C_M$  than in  $C_D$ . This may partly account for the greater relative standard deviation of  $C_D$  (38 per cent of the mean) as compared with that of  $C_M$  (25 per cent of the mean).

The values of  $S_e$  and  $r$  give a quantitative measure of the degree of compatibility of the fitted reaction  $R_1'(t)$  with the sequences of  $R_1^*-A$ . However, a visual comparison of these sequences is quite helpful. Such a comparison is given for each run in Figs. 13 to 16. The full curve in each graph represents the smoothed and adjusted sequence  $R_1^*(t) - A$ , derived from the measurements. The dashed curves represent the fitted reaction  $R_1'(t)$  as given by Eq.(46) using the individual regression coefficients  $C_D$  and  $C_M$  from each run. The dotted curves are plots of the relation

---

<sup>5</sup> The percentages given in the earlier technical report (Reid, 1956, p.46) were found to be in error.

## COASTAL ENGINEERING

$$R_1''(t) = \bar{C}_D F_1^*(t) + \bar{C}_M F_2^*(t) \quad (62)$$

where  $\bar{C}_D$  and  $\bar{C}_M$  are the overall mean values 0.53 and 1.47 respectively

Runs 6 and 9 which are depicted in the lower graph of Fig. 16 were not included in the summary of Table V. The sequences of measured  $R_1$  were too short to subject to the filtering procedure, and consequently no attempt was made to estimate the individual  $C_D$  and  $C_M$  values for these runs. However, adequate water level records were available which permitted the evaluation of the  $F_1$  and  $F_2$  functions. As a test of the regression equation the coefficients  $\bar{C}_D$  and  $\bar{C}_M$  determined from the other runs were employed to compute  $R_1''(t)$  for runs 6 and 9. Thus the dotted curves in the graphs for these runs actually represent predictions of the force from the measured water level. Note that the full curves in these two runs are the unfiltered sequences of measured reaction, unadjusted for true zero reaction.

### 9. CONCLUSIONS

The regression equation (46), using the numerical transformations of  $\eta(t)$  to simulate the field of motion of the fluid, as predicted by the linear wave theory for long crested waves, and assuming drag and inertial coefficients which are independent of velocity and acceleration, allows a reasonably good fit of the measured irregular reactions from which vibrations have been effected. The variation of the individual  $C_D$  and  $C_M$  values, deduced by least square regression techniques for each run, vary considerably from one run to another. However, even when the overall mean values of these coefficients are utilized to predict the reactions the agreement is still surprisingly reasonable. If the individual  $C_D$  and  $C_M$  values are employed for each run, then all but 13 per cent of the variance of  $R_1^*$  can be explained by the drag and inertial forces. It can be shown that  $S_e^2$  is approximately doubled when the overall mean values of the coefficients are used to predict the reaction (dotted curves of Figs. 13 to 16), and the correlation consequently drops from 0.93 to 0.85 for all runs as a whole. This correlation is about the same as that obtained for the individual regression curves for runs 1, 12 and 15.

It would appear that some amount of freedom exists in the possible combinations of  $C_D$  and  $C_M$  which will lead to nearly the same prediction for total load. It may be noted that the sum of the mean  $C_D$  and  $C_M$  values is 2.00. An analysis of the values of  $C_D + C_M$  for each run indicates a standard deviation from the mean which is only 13 per cent of the mean. This may be compared with the standard deviations of the values of  $C_D$  and  $C_M$  separately, which are 38 per cent and 25 per cent of the mean  $C_D$  and  $C_M$  respectively. It is particularly interesting, though undoubtedly somewhat accidental, that the mean sum of the coefficients is 2.00, for this is the value of  $C_M$  which should exist for accelerated irrotational flow around a circular cylinder in the complete absence of a turbulent vortex wake i.e.,

# CORRELATION OF WATER LEVEL VARIATIONS WITH WAVE FORCES ON A VERTICAL PILE FOR NONPERIODIC WAVES

for  $C_D = 0$  (see Lamb, 1945, pp. 75-77). The implication of the above line of reasoning is of course purely conjectural at this stage, but it would appear that for general flow conditions in the presence of turbulence the sum of  $C_D$  and  $C_M$  is more nearly conserved than are the individual coefficients. It would be of interest to test this hypothesis, or some modification thereof in further studies.

The scatter of  $C_D$  and  $C_M$  values obtained from the individual runs are bound to exist in the presence of errors in measurement of  $\eta$  and/or  $R_1$ , or errors in simultaneity of the time sequences, or errors in the estimated subsurface values of steady current. It is also possible and quite likely for the tests reported here that a major source of scatter in the regression coefficients results from the short-crestedness of the waves. The source of difficulty stems from the fact that we have attempted to evaluate a vector force from the measurement of a scalar quantity  $\eta$ . This is legitimate if the waves are long-crested and the reaction which we are attempting to predict is aligned with the wave direction. However, in the presence of short-crested waves there can exist variations in  $\eta$  at the test pile which are related to waves approaching normal to the direction of the predominant waves. These waves could produce little if any reaction in the direction of the predominant waves, and consequently the functions,  $F_1$  and  $F_2$  deduced from such variations in  $\eta$  would be in error. In addition, it was assumed that no reflection of wave energy occurs at the test pile where the measurements of  $\eta$  were made. The effect of the presence of the pile on the waves should be small for long wave lengths, but may have a significant effect for waves of 5 feet in length or shorter (corresponding to one second period or less). The spectral components of 1.6 second and less were filtered from the records in the final analysis, however there could still be some error introduced in the  $F_1$  function by the nonlinearity.

It is considered that the majority of the scatter in the  $C_D$  and  $C_M$  values is a result of the short-crestedness of the waves. In view of the possible errors introduced by short-crestedness it is all the more surprising that the overall mean  $C_D$  and  $C_M$  (0.53 and 1.47 respectively) can lead to a reproduction of the measured reactions with a correlation as high as 0.85.

## 10. ACKNOWLEDGEMENTS

This work represents the results of research carried out under the sponsorship of the U.S. Naval Civil Engineering Research and Evaluation Laboratory of the Bureau of Yards and Docks, Contract NOy-27474, through the Texas A. & M. Research Foundation. The Gulf Coast Division of the Sun Oil Company provided space on the Sun Oil pier at Caplen, Texas and cooperated in many other respects in the measurement phase of the program. The instrumentation and measurements of wave forces were made possible through the efforts of C.L. Bretschneider, G.L. Huebner, and W.H. Clayton. The author is particularly indebted to R.L. Smith for programming and analysis

## COASTAL ENGINEERING

of the numerical data by means of an IBM 650 digital computer, and to R.G. Dean for his assistance in the overall analysis work. Finally, the encouragement and many valuable suggestions of B.W. Wilson must be noted; and certainly Randolph Blumberg deserves much of the credit for the method of analysis of the complex records.

### REFERENCES

1. Fuchs, R.A., (1952), Prediction of Linear Effects from Instrument Records of Wave Motion, Tech. Report Ser. 3, Issue 337, Inst. of Engr. Res., Univ. of Calif., Berkeley, 8 pp. 1952 (unpublished).
2. Lamb, Horace, (1945), Hydrodynamics, Dover Publ., New York, 738 pp., 1945.
3. Longuet-Higgins, M.S., (1952), On The Statistical Distribution of The Heights of Sea Waves, Journ. Mar. Res., V. 11, pp. 245-266, 1952.
4. Morison, J.R., O'Brien, M.P., Johnson, J.W., and Schaaf, S.A., (1950), The Force Exerted by Surface Waves on Piles, Petroleum Trans., Amer. Inst. Mining Engineers, V.189, pp. 149-154, 1950.
5. Reid, R.O., (1954), Wave Force Experiments at Atchafalaya Bay, Louisiana (Pure Oil Company Platform), Tech. Report No. 38-1, Dept. of Oceanography, A. & M. College of Texas, 56 pp., Feb., 1954 (unpublished).
6. Reid, R.O., (1956), Analysis of Wave Force Experiments at Caplen, Texas (Sun Oil Company Platform), Final Report No. 38-4, Ref. 56-2 Dept. of Oceanography, A. & M. College of Texas, 49 pp., January, 1956 (unpublished).
7. Wiegel, R.L., and Kukk, J., (1957), Wave Measurements Along The California Coast, Trans. Amer. Geoph. Union, V. 38, n. 5, pp. 667-674, October, 1957.
8. Wiener, Norbert, (1950), Extrapolation, Interpolation, and Smoothing of Stationary Time Series, John Wiley and Sons, Inc., New York, 163 pp., 1950.
9. Wilson, B.W., and Reid, R.O., (1955), Effect of Vibration on the Measurement of Wave Forces, Tech. Report No. 38-2, Ref. 55-41T, Dept. of Oceanography, A. & M. College of Texas, 42 pp., December 1955 (unpublished).